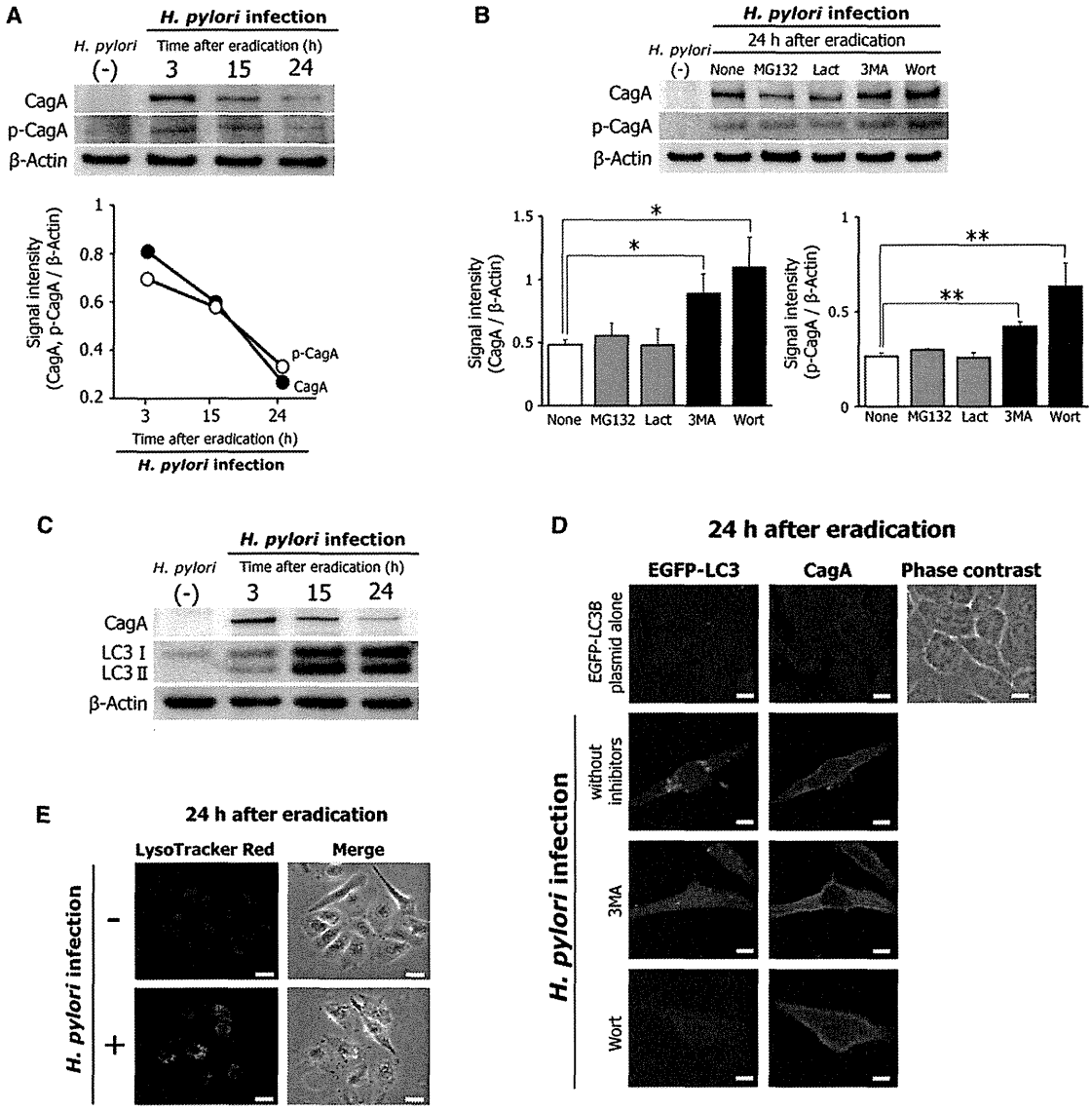

Figure 1. Autophagy Induction Associated with Intracellular CagA Stability

(A) AGS cells infected with *H. pylori* ATCC700392 for 5 hr were incubated at indicated times in a medium containing antibiotic to kill extracellular bacteria. Intracellular CagA and phosphorylated CagA (p-CagA) levels were quantified. Data represent the mean of three independent assays.

(B) AGS cells infected with *H. pylori* for 5 hr were incubated in a medium containing antibiotic with or without a proteasome inhibitor (10 μM MG132 or 20 μM lactacystin [Lact]) or autophagy inhibitor (5 mM 3-methyladenine [3MA] or 50 nM wortmannin [Wort]) for 24 hr. Intracellular CagA and p-CagA levels were quantified. Data represent the mean ± SD of three independent assays; *$p < 0.05$, **$p < 0.01$.

(C) AGS cells infected with *H. pylori* ATCC700392 for 5 hr were incubated in a medium containing antibiotic for the indicated times, and intracellular CagA and LC3-I to LC3-II conversion were examined.

(D) After transfection of AGS cells with the EGFP-LC3B plasmid, cells infected with *H. pylori* for 5 hr were incubated with a medium containing antibiotic for 24 hr with or without an autophagy inhibitor (10 μM MG132 or 20 μM Lact), and intracellular CagA was stained. EGFP-LC3B plasmid alone indicates the absence of *H. pylori* infection. Scale bar = 25 μm.

(E) AGS cells infected with *H. pylori* ATCC700392 for 5 hr were incubated with a medium containing antibiotic for 24 hr, and LysoTracker Red DND-99 staining was performed. Scale bar = 50 μm.

not affected by proteasome inhibitors (10 μM MG132 or 20 μM Lact), they were significantly increased by exposure of the cells to autophagy inhibitors (5 mM 3MA or 50 nM Wort), as compared with cells not exposed to these inhibitors (None) (Figure 1B). These results indicated that autophagy contributed to CagA degradation in host epithelial cells.

We then examined whether autophagy was activated within AGS cells after *H. pylori* ATCC700392 eradication. A hallmark of autophagy is the carboxyl terminus modification of microtubule-associated protein light chain 3 (LC3), which becomes linked to phosphatidylethanolamine and associates with the autophagosomal membrane. LC3-I to LC3-II conversion was

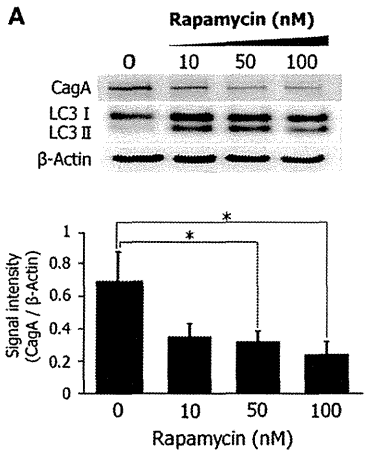

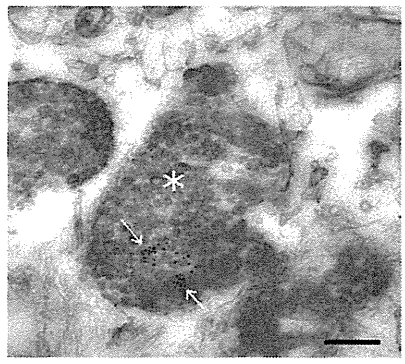

Figure 2. Degradation of Intracellular CagA by the Induction of Autophagy

(A) CagA expression in WT-A10 cells was induced by removal of Dox for 24 hr (CagA-expressing WT-A10 cells). CagA-expressing WT-A10 cells were stimulated with rapamycin for 24 hr, and intracellular CagA and LC3-I to LC3-II conversion were examined. Data represent the mean ± SD of three independent assays; *$p < 0.05$.

(B) CagA-expressing WT-A10 cells stimulated with 100 nM rapamycin for 24 hr were reacted with a 15 nm immunogold-labeled antibody; immunogold-labeled CagA was detected by electron microscopy. Arrows indicate immunogold-labeled CagA. Label is autophagolysosomal components. Scale bar = 200 nm.

detected most clearly at 15 and 24 hr after *H. pylori* eradication (Figure 1C). In addition, 24 hr after eradication, EGFP-LC3B-positive puncta were clearly detected within the cytoplasm of AGS cells transfected with the EGFP-LC3B plasmid, unlike AGS cells exposed to autophagy inhibitors (5 mM 3MA, 50 nM Wort) (Figure 1D), suggesting that LC3 is activated and localized to autophagosomes. LysoTracker Red stains late autophagic vacuoles (autolysosomes), but not early autophagosomes. LysoTracker Red staining was clearly detected within AGS cells at 24 hr after *H. pylori* eradication, consistent with the formation of autolysosomes (Figure 1E). These results demonstrate that autophagy was activated in AGS cells at 15 and 24 hr after eradication.

To evaluate whether autophagy was specifically associated with degradation of intracellular CagA, CagA-expressing WT-A10 cells—in which CagA expression was induced through the pTet-off-*cagA* expression vector by the absence of doxycycline (Dox) for 24 hr—was used. When these cells were incubated with rapamycin, which promotes autophagy by inhibiting mammalian target of rapamycin (mTOR), intracellular CagA decreased in a dose-dependent manner, and LC3-I to LC3-II conversion was clearly detected (Figure 2A). In addition, electron immunocytochemical examination following immunogold labeling for CagA in CagA-expressing, rapamycin-stimulated WT-A10 cells revealed the presence of labeled CagA in autophagic vesicles (Figure 2B). From these results, we conclude that intracellular CagA is degraded by autophagy.

CagA Degradation via Autophagy Is Activated by m1VacA

Although autophagy was activated in AGS cells after *H. pylori* eradication (Figures 1C–1E), no LC3-I to LC3-II conversion was detected in CagA-expressing WT-A10 cells without rapamycin (Figure 2A; rapamycin [0 nM] lane). These results indicate that the induction of autophagy was independent of intracellular CagA, but was dependent on *H. pylori* infection. According to Terebiznik et al. (2009), autophagy was induced by VacA in *H. pylori*-infected AGS cells; therefore, we tested whether VacA participated in induction of autophagy associated with CagA degradation. In CagA-expressing WT-A10 cells exposed to culture supernatant from *H. pylori* ATCC700392 (s1m1VacA), intracellular CagA levels were significantly decreased in the culture supernatant in a dose-dependent manner with LC3-I to LC3-II conversion (Figure 3A). In addition, in AGS cells at 24 hr after *H. pylori* ATCC700392 (s1m1VacA) eradication, intracellular CagA levels were significantly decreased, as compared to 15 hr after eradication; conversion of LC3-I to LC3-II was clearly evident (Figure 3B). Conversely, in WT-A10 cells exposed to *H. pylori* F57 (VacA-negative), ot210 (s1m2VacA), or SS1 (s2m2VacA) culture supernatant, there was no decrease in intracellular CagA levels, and no LC3-I to LC3-II conversion was detected (Figure S1A). Moreover, in AGS cells at 24 hr after *H. pylori* F57 (VacA-negative), ot210 (s1m2VacA), or SS1 (s2m2VacA) eradication, there was no decrease in intracellular CagA, and no LC3-I to LC3-II conversion was detected (Figure S1B). To investigate the function of CagA from each strain, we examined the tyrosine phosphorylation level of each CagA protein. All the CagA proteins were phosphorylated (Figure S1C), suggesting that those CagA species behaved similarly in delivered host cells.

In CagA-expressing WT-A10 cells incubated with m1VacA for 24 hr, a significant m1VacA-dependent decrease in intracellular CagA levels was observed along with LC3-I to LC3-II conversion (Figure 3C). Autophagy inhibitors (5 mM 3MA or 50 nM Wort) repressed the LC3-I to LC3-II conversion induced by m1VacA and significantly increased intracellular CagA levels (Figure 3D). In CagA-expressing WT-A10 cells incubated with m2VacA, intracellular CagA was not degraded and LC3-I to LC3-II conversion was not observed (Figure S1D). In addition, at 24 hr after *H. pylori* F57 (VacA-negative) eradication, there was a significant increase in CagA, as compared with cells infected with *H. pylori* ATCC700392 (s1m1VacA) (Figure S1E). The increase of intracellular CagA produced by *H. pylori* F57 (VacA-negative) was reduced by the addition of 60 nM m1VacA, in contrast to the addition of 60 nM m2VacA (Figure S1E). To evaluate the biological activity of VacA, we examined the vacuolation activity of m1VacA and m2VacA. Both proteins induced vacuolation in CagA-expressing WT-A10 cells in a dose-dependent manner, although m1VacA induced stronger vacuolation activity than m2VacA (Figure S1F). Our observations demonstrate that the autophagy responsible for CagA degradation is induced by m1VacA in gastric epithelial cells, independent of vacuolating cytotoxicity.

We recently found that low-density lipoprotein receptor-related protein-1 (LRP1) was one of the VacA receptors that

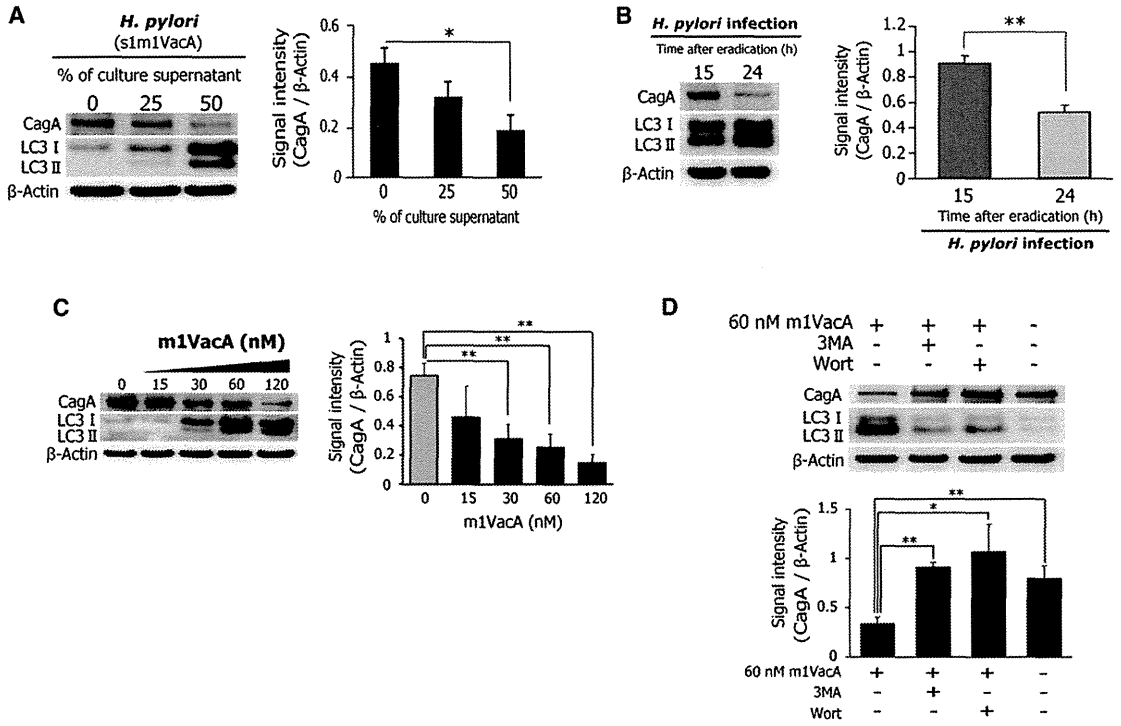

Figure 3. Autophagy, Causing CagA Degradation, Is Induced by m1VacA

(A) CagA-expressing WT-A10 cells were stimulated with *H. pylori* ATCC700392 (s1m1VacA) culture supernatant, and intracellular CagA and LC3-I to LC3-II conversion were examined. Data represent the mean ± SD of three independent assays; *p < 0.05.

(B) AGS cells infected with *H. pylori* (s1m1VacA) for 5 hr were incubated in a medium containing antibiotic for 15 and 24 hr, and intracellular CagA and LC3-I to LC3-II conversion were examined. Data represent the mean ± SD of three independent assays; **p < 0.01.

(C) CagA-expressing WT-A10 cells were incubated with m1VacA for 24 hr, and intracellular CagA and LC3-I to LC3-II conversion were examined. Data represent the mean ± SD of three independent assays; **p < 0.01.

(D) CagA-expressing WT-A10 cells, stimulated by m1VacA, were incubated with an autophagy inhibitor (5 mM 3MA or 50 nM Wort) for 24 hr, and intracellular CagA and LC3-I to LC3-II conversion were examined. Data represent the mean ± SD of three independent assays; *p < 0.05, **p < 0.01. See also Figure S1.

mediate induction of autophagy (Yahiro et al., 2012). Then, to examine the relevance of LRP1 for the induction of autophagy-mediated CagA degradation, we constructed specific LRP1-knockdown AGS cells using small interfering RNAs (siRNAs) (Figure S1G). The LRP1 knockdown repressed the LC3-I to LC3-II conversion, resulting in the inhibition of CagA degradation (Figure S1H). This result indicates that LRP1 is required for the induction of autophagy-mediated CagA degradation in response to m1VacA. Next, to compare the binding ability of m1VacA and m2VacA to LRP1, we performed an immunoprecipitation assay with anti-LRP1. An 87 kDa fragment of VacA was detected by western blotting with an anti-VacA antibody in the anti-LRP1 immunoprecipitates from AGS cells infected with *H. pylori* ATCC700392 (s1m1VacA) (Figure S1I). In contrast, VacA was not detected in the anti-LRP1 immunoprecipitates from AGS cells infected with *H. pylori* ot210 (s1m2VacA) (Figure S1I). This result demonstrates that m1VacA, but not m2VacA, has a binding potential to LRP1.

p53 Downregulation via Increased MDM2-Phosphorylation Induces Autophagy, Causing CagA Degradation

p53 inactivation by chemical inhibition or knockdown induces autophagy via the inhibition of mTOR. To investigate the induction of autophagy associated with CagA degradation, we examined p53 expression in AGS cells after *H. pylori* infection. In AGS cells at 15 and 24 hr after eradication of *H. pylori* ATCC700392 (s1m1VacA), p53 expression was significantly decreased and LC3-I to LC3-II conversion was clearly detected (Figure 4A). We then examined the mechanisms of p53 downregulation, focusing on posttranslational mechanisms, since *H. pylori*-infected AGS cells have been reported to show no change in *p53* mRNA expression (Wei et al., 2010). It is well known that p53 can be degraded by ubiquitination and proteasomal degradation pathways and that murine double minute 2 (MDM2) is the main E3 ubiquitin ligase that mediates p53 degradation. MDM2 expression was unaltered in AGS cells after *H. pylori* ATCC700392 (s1m1VacA) infection (Figure 4B). MDM2 is activated by phosphorylation at Ser166 (pMDM2) (Zhou et al., 2001). At 15 and 24 hr after the eradication of *H. pylori* ATCC700392 (s1m1VacA), pMDM2 levels were significantly increased (Figure 4B). Conversely, in AGS cells after *H. pylori* F57 (VacA-negative), ot210 (s1m2VacA), or SS1 (s2m2VacA) infection, neither a decrease in p53 expression nor an increase in pMDM2 was noted (Figure S2).

We then examined the relationship between p53 downregulation and intracellular CagA stability. The specific

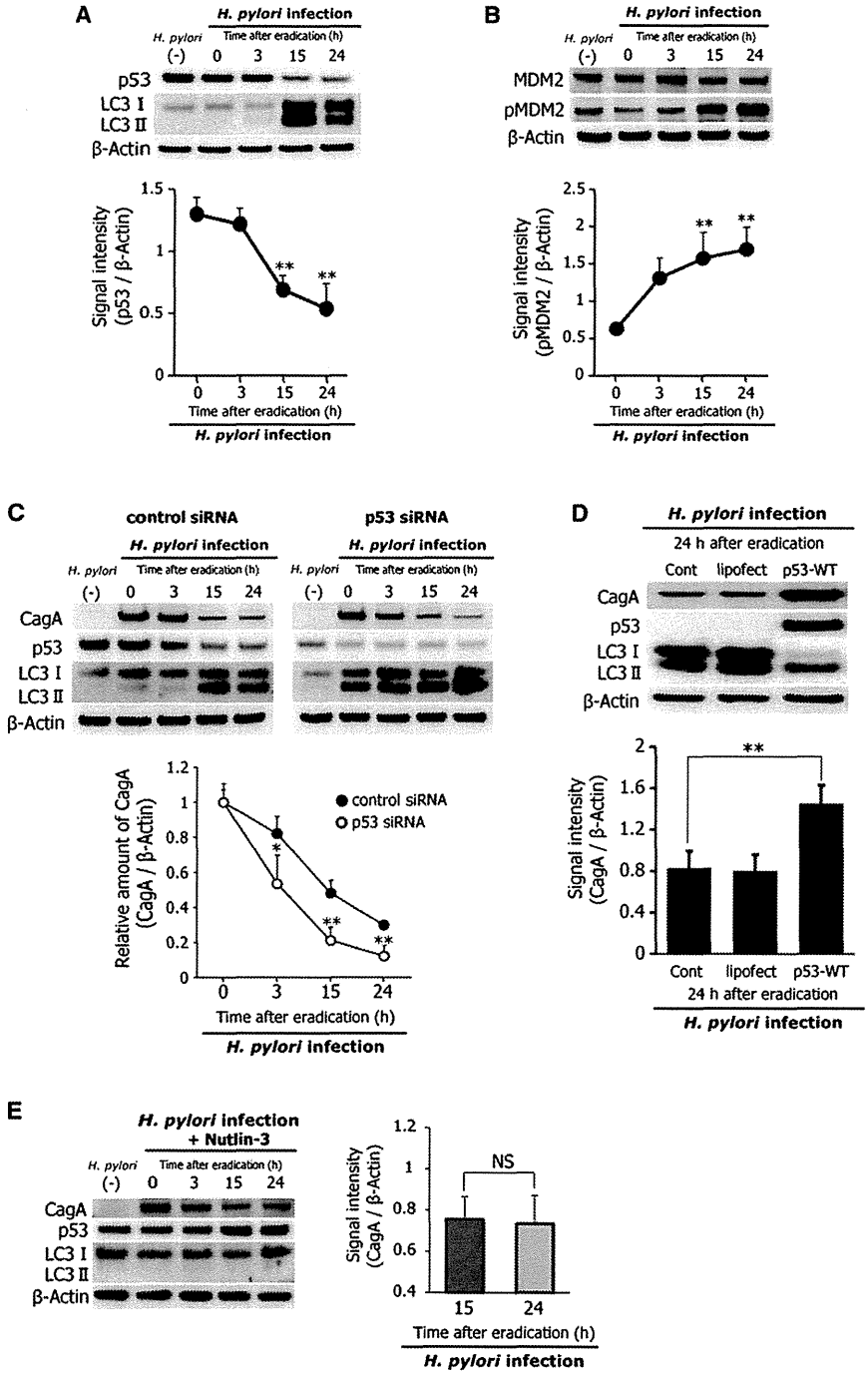

Figure 4. Autophagy, Causing CagA Degradation, Is Induced through MDM2-Mediated p53 Degradation

(A) AGS cells infected with *H. pylori* (s1m1VacA) for 5 hr were incubated in a medium containing antibiotic for the indicated time, and p53 expression and LC3-I to LC3-II conversion were examined. Data represent the mean ± SD of three independent assays; $^{**}p < 0.01$, compared to AGS cells at 0 hr after *H. pylori* (s1m1VacA) eradication.

(B) AGS cells infected with *H. pylori* (s1m1VacA) for 5 hr were incubated in a medium containing antibiotic for the indicated times, and the levels of MDM2 and phosphorylated-MDM2 (pMDM2) were examined. Data represent the mean ± SD of three independent assays; $^{**}p < 0.01$, compared to AGS cells at 0 hr after *H. pylori* (s1m1VacA) eradication.

(C) After AGS cells were transfected with control siRNA or p53 siRNA, cells infected with *H. pylori* (s1m1VacA) for 5 hr were incubated in a medium containing antibiotic for the indicated times, and the levels of CagA, p53 expression, and LC3-I to LC3-II conversion were examined. Data represent the mean ± SD of three independent assays; $^{**}p < 0.01$, compared to AGS cells transfected with control siRNA at each time point after *H. pylori* (s1m1VacA) eradication.

(D) KATOIII cells were transfected with the pCMV-Neo-Bam WT *p53* plasmid (p53-WT) or without (Cont). Each cell after *H. pylori* (s1m1VacA) infection for 5 hr was incubated in a medium containing antibiotic for the indicated times. CagA levels and LC3-I to LC3-II conversion were examined. Data represent the mean ± SD of three independent assays; $^{**}p < 0.01$; lipofect indicates KATOIII cells treated with only Lipofectamine 2000.

(E) AGS cells infected with *H. pylori* (s1m1VacA) for 5 hr were incubated in a medium containing antibiotic for the indicated times with 10 μM nutlin-3, and the levels of CagA, p53 expression, and LC3-I to LC3-II conversion were examined. Data represent the mean ± SD of three independent assays; NS, not significant. See also Figure S2.

p53-knockdown using small interfering RNAs (siRNAs) accelerated LC3-I to LC3-II conversion, thereby enhancing CagA degradation in AGS cells after *H. pylori* ATCC700392 (s1m1VacA) infection (Figure 4C). Moreover, in KATOIII cells, which are genetically deficient of p53 ($p53^{-/-}$ KATOIII cells), LC3-I to LC3-II conversion was clearly detected at 24 hr after the eradication of *H. pylori* ATCC700392 (s1m1VacA), and intracellular CagA levels were significantly decreased, as compared with $p53^{-/-}$ KATOIII cells transfected with the WT *p53* expression plasmid (Figure 4D). In addition, we examined the effect of nutlin-3—an inhibitor of MDM2-phosphorylation—on CagA stability. Treatment with 10 μM nutlin-3 repressed p53 downregulation and LC3-I to LC3-II conversion (Figure 4E), resulting in the inhibition of CagA degradation (Figure 4E). These results show that p53 downregulation, through the acceleration of MDM2-phosphorylation by m1VacA, induces autophagy, causing CagA degradation.

ROS Accumulation Is Necessary for the Induction of Autophagy, Causing CagA Degradation

An accumulation of intracellular ROS induces autophagy, and the generation of intracellular ROS is enhanced in gastric epithelial cells during *H. pylori* infection (Ding et al., 2007). We hypothesized that the enhanced generation of intracellular ROS participates in induction of autophagy, causing CagA

degradation. AGS cells at 15 and 24 hr after the eradication of infected *H. pylori* were analyzed using fluorescence microscopy and flow cytometry after staining with CM-H_2DCFDA, an ROS-sensitive fluorescent probe. Hydrolyzed CM-H_2DCFDA is oxidized to dichlorofluorescein (DCF) by intracellular ROS (Suzuki et al., 1994). DCF fluorescence was apparent in AGS cells at 15 and 24 hr after the eradication of *H. pylori* ATCC700392 (s1m1VacA), as compared with AGS cells without *H. pylori* exposure (Figure 5A). The intensity of DCF fluorescence in AGS cells at 15 and 24 hr after the eradication of *H. pylori* ATCC700392 (s1m1VacA) was significantly increased, as compared to AGS cells without *H. pylori* exposure (Figure 5B). Conversely, in AGS cells after *H. pylori* F57 (VacA-negative), ot210 (s1m2VacA), or SS1 (s2m2VacA) infection, no increase in DCF fluorescence was observed (Figure S3A). These results show that the accumulation of intracellular ROS was enhanced during the induction of autophagy.

NADPH oxidase (NOX)-generated ROS is a key regulator of autophagy (Huang et al., 2009), while mitochondrial-superoxide (O_2^-) production is involved in the induction of autophagy (Scherz-Shouval and Elazar, 2007). To identify the source of enhanced ROS generation associated with the induction of autophagy through p53 downregulation, we examined the effects of an NOX inhibitor (acetovanillone), an MnSOD mimic compound (MnTMPyP), and N-acetylcysteine (NAC). p53 downregulation was not inhibited by 250 μM acetovanillone or 20 μM MnTMPyP; therefore, LC3-I to LC3-II conversion was not repressed (Figure 5C). Conversely, p53 downregulation was inhibited by treatment with 10 mM NAC, and LC3-I to LC3-II conversion was repressed (Figure 5C). Moreover, intracellular CagA levels were significantly increased by treatment of AGS cells with 10 mM NAC at 24 hr after the eradication of *H. pylori* ATCC700392 (s1m1VacA) (Figure 5D). These results show that the accumulation of intracellular ROS is necessary for induction of autophagy, causing CagA degradation, independent of NOX- and mitochondria-associated ROS generation.

Administration of NAC, a cysteine prodrug, replenishes intracellular GSH levels; therefore, NAC has been used to treat GSH deficiency (Atkuri et al., 2007). We hypothesized that the accumulation of intracellular ROS during the induction of autophagy was caused by decreased GSH levels. To prove this, we examined the change of GSH levels in AGS cells after *H. pylori* ATCC700392 (s1m1VacA) infection. Intracellular GSH levels in AGS cells at 15 and 24 hr after the eradication of *H. pylori* ATCC700392 (s1m1VacA) were significantly decreased, as compared to AGS cells without *H. pylori* exposure (Figure 5E). Moreover, intracellular GSH levels in AGS and CagA-expressing WT-A10 cells were significantly decreased by m1VacA in a dose-dependent manner (Figure 5F). In AGS cells at 15 and 24 hr after the eradication of *H. pylori* ATCC700392 (s1m1VacA), intracellular GSH was decreased, as compared to cells at 15 and 24 hr after eradication of *H. pylori* F57 (VacA-negative), ot210 (s1m2VacA), or SS1 (s2m2VacA) (Figure S3B). Moreover, intracellular GSH levels in AGS and CagA-expressing WT-A10 cells were not decreased by treatment with m2VacA (Figure S3C). These results show that the accumulation of intracellular ROS associated with the induction of autophagy was induced by decreased GSH levels caused by m1VacA. Next, to provide the relevance of LRP1 in the reduction of intracellular GSH levels, we measured intracellular GSH levels in specific LRP1-knockdown AGS cells; they were significantly increased at 15 or 24 hr after the eradication of *H. pylori* ATCC700392 (s1m1VacA), as compared with those in AGS cells transfected with control siRNA (Figure S3D). These results demonstrate that the binding of m1VacA to LRP1 is required for the reduction of intracellular GSH levels.

Activation of the Akt Pathway Depends on the Accumulation of ROS for Autophagy Induction

Phosphorylated Akt enhances the ubiquitination-promoting function of MDM2 by phosphorylation, resulting in p53 downregulation (Ogawara et al., 2002). In addition, exogenous and endogenous ROS enhance Akt phosphorylation (Dong-Yun et al., 2003). We hypothesized that the accumulation of intracellular ROS by decreased GSH levels enhances Akt phosphorylation, leading to the induction of autophagy through p53 downregulation by the activation of MDM2. To investigate this hypothesis, we examined Akt phosphorylation in AGS cells after *H. pylori* ATCC700392 (s1m1VacA) infection. Although Akt expression was unaltered, the levels of phosphorylated Akt at Thr308 and Ser473 were significantly increased in AGS cells after *H. pylori* ATCC700392 (s1m1VacA) infection (Figure 6A). To examine whether Akt phosphorylation depends on the accumulation of intracellular ROS, we examined the effect of NAC on Akt phosphorylation. Treatment with 10 mM NAC inhibited Akt phosphorylation at Ser473, but not at Thr308 (Figure 6A); therefore, Akt phosphorylation at Ser473 was dependent on accumulation of intracellular ROS after *H. pylori* ATCC700392 (s1m1VacA) infection. In addition, although Akt phosphorylation at Thr308 was increased in AGS cells after *H. pylori* F57 (VacA-negative), ot210 (s1m2VacA), or SS1 (s2m2VacA) infection, Akt phosphorylation at Ser473 was not increased (Figure S4A). Moreover, Akt phosphorylation at Thr308 and Ser473 was not increased in CagA-expressing WT-A10 cells, suggesting that Akt phosphorylation was independent of intracellular CagA (Figure S4B).

To examine the relevance of Akt phosphorylation at Ser473 to the induction of autophagy, causing CagA degradation, we examined the effect of LY294002, an inhibitor of Akt phosphorylation, on the stability of intracellular CagA and autophagy induction. Ten micromolar LY294002 inhibited intracellular CagA degradation, the increase in pMDM2, and p53 downregulation (Figure 6B). As a result, LC3-I to LC3-II conversion in AGS cells at 15 and 24 hr after the eradication of *H. pylori* ATCC700392 (s1m1VacA) was repressed by LY294002 with reduced accumulation of LysoTracker Red (Figure 6C). These results suggest that enhanced Akt phosphorylation at Ser473 induced MDM2 phosphorylation, leading to the induction of autophagy and causing CagA degradation through p53 downregulation.

Accumulation of Translocated CagA in CD44v9-Expressing Gastric Cancer Stem-like Cells

Intracellular CagA produced by m1VacA *H. pylori*, but not m2VacA *H. pylori*, was degraded by autophagy. Although some studies indicated that m1VacA *H. pylori* infection was at a greater risk of gastric cancer compared with m2VacA *H. pylori* infection (Basso et al., 2008; Miehlke et al., 2000), others have indicated that there is no correlation between virulence and the *vacA*

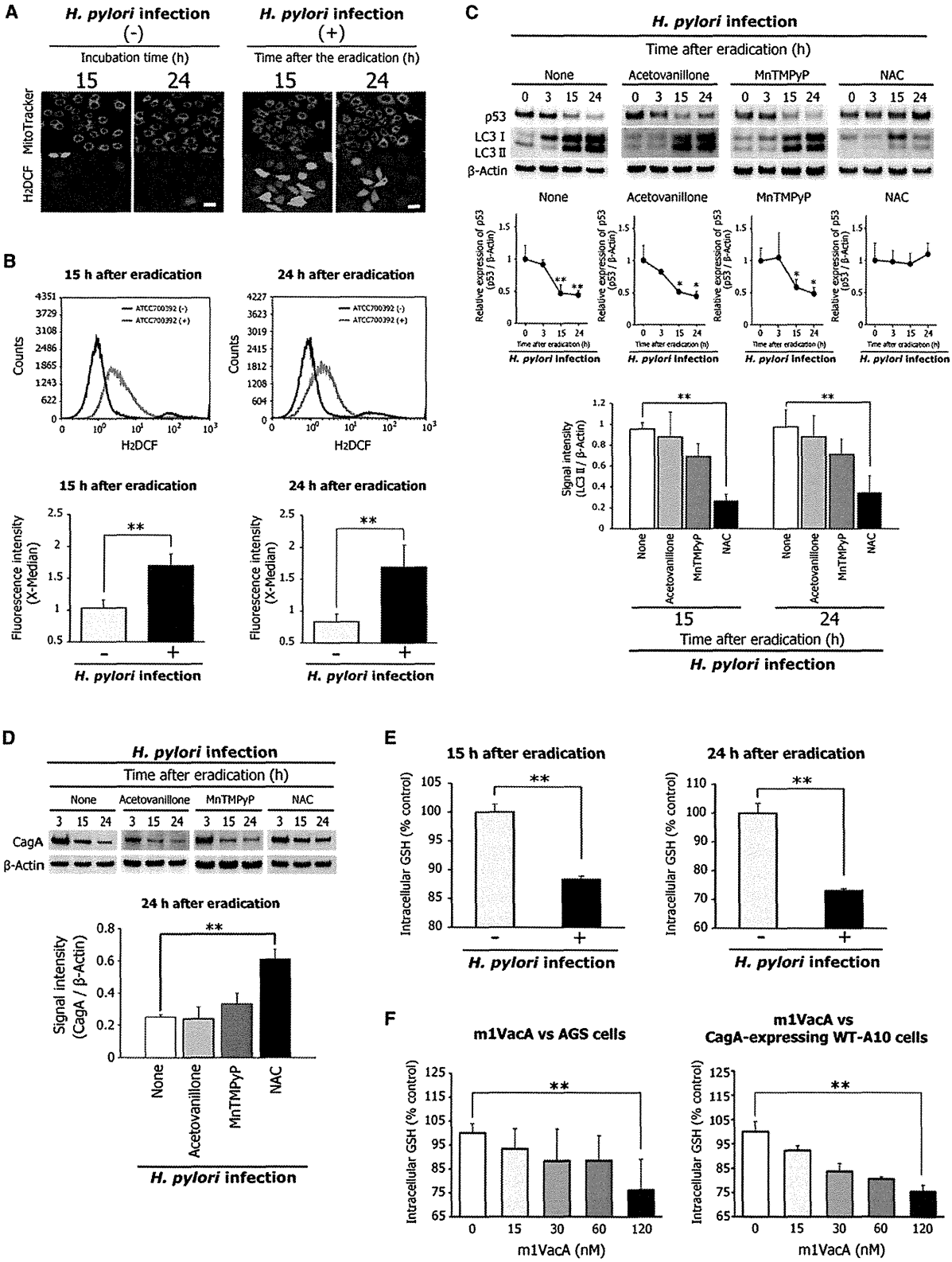

Figure 5. Reduced Intracellular GSH Levels Trigger Autophagy, Causing CagA Degradation

(A) AGS cells at 24 hr after *H. pylori* (s1m1VacA) eradication were stained with CM-H_2DCFDA and MitoTracker Red FM and examined by fluorescence microscopy. Scale bar = 50 μm.

(B) Flow cytometry of AGS cells at 15 and 24 hr after *H. pylori* (s1m1VacA) eradication. H_2DCF fluorescence intensity was determined by using analysis software. Data represent the mean ± SD of three independent assays; $^{**}p < 0.01$.

genotype (Marshall et al., 1999; Yamaoka et al., 1998). In fact, m1 and m2 VacA strains are both observed in gastric cancer patients (Wang et al., 1998). From these reports, we hypothesized that there was a characteristic alteration in host cell associated with the inhibition of autophagy, which led to the accumulation of intracellular CagA. CD44v9-expressing gastric cancer cells are resistant to ROS, supported by increased intracellular GSH synthesis (Ishimoto et al., 2011). We hypothesized that accumulation of intracellular CagA resulted from inhibiting autophagy induction in CD44v9-expressing cells. To prove this hypothesis, we prepared MKN28 mutant cells by transfection of CD44 standard form (CD44s)- or CD44v9-expression vectors into CD44-negative MKN28 cells (Ishimoto et al., 2011). CD44s or CD44v9 expression in MKN28 cells was confirmed using flow cytometry (Figure S5A). Intracellular GSH levels in MKN28 cells expressing CD44s were significantly increased in comparison to MKN28 cells, whereas GSH levels in MKN28 cells expressing CD44v9 were increased in comparison to MKN28 cells expressing CD44s (Figure S5B). These results were consistent with previous observations that CD44v9 expression increases cellular GSH contents through the promotion of xCT-mediated cystine uptake, and CD44s expression increases cellular GSH levels through the maintenance of pentose phosphate pathway (PPP) flux and consequent NADPH production (Tamada et al., 2012). Intracellular GSH levels in MKN28 cells expressing CD44v9 were not decreased at 15 or 24 hr after the eradication of *H. pylori* ATCC700392 (s1m1VacA), in contrast to the reduction of GSH levels in MKN28 cells expressing CD44s (Figure 7A). Intracellular CagA levels were significantly increased in MKN28 cells expressing CD44v9, as compared with those in MKN28 cells expressing CD44s (Figure 7B). In addition, the increase of Akt and MDM2 phosphorylation and p53 degradation were not observed in MKN28 cells expressing CD44v9 (Figure 7B). As a result, LC3-I to LC3-II conversion was repressed (Figure 7B) and LysoTracker signals were markedly decreased in MKN28 cells expressing CD44v9 (Figure 7C). These results suggest that intracellular CagA accumulated in cells expressing CD44v9 through the inhibition of autophagy. We then examined the effect of sulfasalazine, a potent xCT inhibitor, on the stability of intracellular CagA in MKN28 cells expressing CD44v9. Intracellular CagA levels were decreased by the application of sulfasalazine in a dose-dependent fashion (Figure 7D). Moreover, Akt and MDM2 phosphorylation was significantly increased, and p53 downregulation was induced by treatment with sulfasalazine (Figure 7D), resulting in a significant increase in the conversion of LC3-I to LC3-II (Figure 7D).

To assess the effect of CD44v9-expression on the accumulation of intracellular CagA in human gastric adenocarcinoma, endoscopically resected early gastric cancer tissue from four patients (case 1: 62-year-old female, well-differentiated adenocarcinoma, *H. pylori*-positive; case 2: 68-year-old male, well-differentiated adenocarcinoma, *H. pylori*-positive; case 3: 72-year-old male, well-differentiated adenocarcinoma, *H. pylori*-positive; case 4: 78-year-old male, well-differentiated adenocarcinoma, *H. pylori*-positive), with written informed consent, was used. Remarkable intracellular CagA staining was detected with an anti-CagA antibody in the CD44v9-positive cells in each gastric adenocarcinoma (Figure 7E). It was confirmed using an anti-*H. pylori* antibody that these CagA-stained patterns were different from *H. pylori*-specific staining (not CagA) (data not shown), suggesting that only transported CagA, but not the *H. pylori* itself, was detected in CD44v9-expressing gastric cancer tissue. Endoscopically resected early gastric cancer tissue from an *H. pylori*-negative patient (80-year-old female, well-differentiated adenocarcinoma), with written informed consent, was used as a CagA-negative control. In this specimen, intracellular CagA staining was not detected in either CD44v9-positive or CD44v9-negative cells (Figure S5C). In addition, we detected the intracellular CagA-negative region in both CD44v9-positive and CD44v9-negative cells in endoscopically resected early gastric cancer tissue from a patient at 40 months after *H. pylori* eradication (72-year-old male, well-differentiated adenocarcinoma), with written informed consent (Figure S5D). In addition to performing a general pathological assessment, LC3B and CD44v9 were stained using fluorescent immunohistochemistry for a paraffin-embedded pathological tissue specimen. In cells expressing CD44v9, there were fewer LC3B-positive puncta than in CD44v9-negative cells, suggesting that autophagy was repressed within the CD44v9-positive cells (Figure 7F). These results indicate that the accumulation of intracellular CagA with autophagy inhibition was confirmed in CD44v9-expressing cancer stem-like cells of human gastric adenocarcinoma.

DISCUSSION

The present study reveals that the accumulation of intracellular CagA in CD44v9-expressing cancer stem-like cells is caused by the repression of autophagy. The autophagic pathway associated with CagA degradation is induced as follows: m1VacA-induced GSH deficiency via binding to LRP1 and then enhances Akt phosphorylation at Ser473. Activation of Akt induces MDM2-mediated p53 degradation through the ubiquitin-proteasome system and then activates autophagy.

Figures S1I and S3D indicated that binding of m1VacA to LRP1 was required for the reduction of intracellular GSH levels and the induction of autophagy, causing CagA degradation. In contrast,

(C) AGS cells infected with *H. pylori* (s1m1VacA) for 5 hr were incubated in a medium containing antibiotic for the indicated times with 250 μM acetovanillone (NOX inhibitor), 20 μM MnTMPyP (MnSOD mimic), or 10 mM NAC. p53 expression and LC3-II formation were examined. Data represent the mean ± SD of three independent assays; *$p < 0.05$, **$p < 0.01$, compared to AGS cells at 0 hr after eradication (p53-expression, middle panel). None indicates without inhibitor.
(D) AGS cells infected with *H. pylori* (s1m1VacA) for 5 hr were incubated in a medium containing antibiotic for the indicated times with 250 μM acetovanillone (NOX inhibitor), 20 μM MnTMPyP (MnSOD mimic), or 10 mM NAC, and intracellular CagA levels were examined. Data represent the mean ± SD of three independent assays; **$p < 0.01$. None indicates without inhibitor.
(E) AGS cells infected with *H. pylori* (s1m1VacA) for 5 hr were incubated in a medium containing antibiotic for 15 and 24 hr, and intracellular GSH levels were measured. Data represent the mean ± SD of three independent assays; **$p < 0.01$.
(F) AGS cells or CagA-expressing WT-A10 cells were incubated with m1VacA for 24 hr, and intracellular GSH levels were measured. Data represent the mean ± SD of three independent assays; **$p < 0.01$. See also Figure S3.

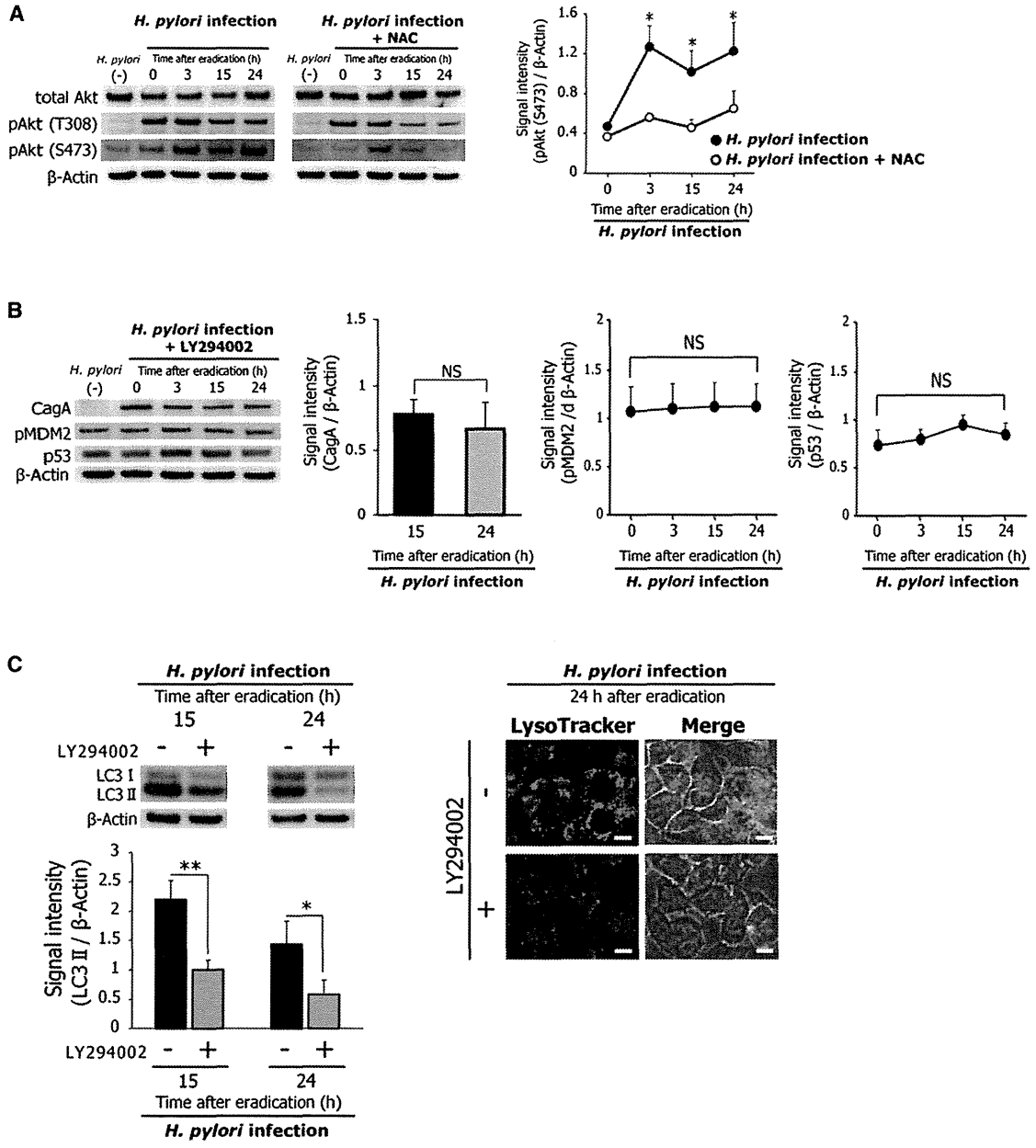

Figure 6. Akt Phosphorylation in Response to Intracellular ROS Accumulation Contributes to Induction of Autophagy, Causing CagA Degradation

(A) AGS cells infected with *H. pylori* for 5 hr were incubated in a medium containing antibiotic for the indicated times, with or without 10 mM NAC. Akt phosphorylation at Thr308 and Ser473 was examined. Data represent the mean ± SD of three independent assays; *p < 0.05, compared to AGS cells at 0 hr after eradication (right panel).

(B) AGS cells infected with *H. pylori* for 5 hr were incubated in a medium containing antibiotic for the indicated time with 10 μM LY294002 (Akt-phosphorylation inhibitor), and the levels of intracellular CagA, pMDM, and p53 were examined. Data represent the mean ± SD of three independent assays; NS, not significant.

(C) AGS cells infected with *H. pylori* for 5 hr were incubated in a medium containing antibiotic for the indicated times with 10 μM LY294002 (Akt-phosphorylation inhibitor), and LC3-II formation was examined. Data represent the mean ± SD of three independent assays; *p < 0.05, **p < 0.01. AGS cells at 24 hr after eradication with or without LY294002 were stained using LysoTracker Red DND-99 (right panel). Scale bar = 50 μm. See also Figure S4.

the binding to LRP1 of m2VacA was not detectable by immunoprecipitation assay (Figure S1I). It has been reported that the mid-region of VacA has an important role in the binding of VacA to host cells (Cover and Blanke, 2005). Therefore, these findings suggest that the reason m2VacA could not induce autophagy was the lack of binding ability to LRP1, unlike m1VacA.

Our observations indicate that m1VacA reduces intracellular CagA levels via the induction of autophagy (Figure 3). Intracellular CagA deregulates SHP-2 and PAR1, which promote cell

proliferation, thus causing loss of cell polarity (Saito et al., 2010). Therefore, an excess of intracellular CagA leads to cell damage that disturbs the attachment of bacteria to gastric epithelial cells. Recently, it was suggested that VacA can downregulate CagA-induced signal-transduction in gastric epithelial cells to some extent, thus minimizing the degree of cellular damage (Yokoyama et al., 2005). Therefore, this CagA degradation response to VacA is considered an important strategy for the long-term colonization of the gastric mucosa by *H. pylori*.

H. pylori ATCC700392-derived CagA contains the EPIYA-ABC motif, and CagA expressed in WT-A10 cells contains the EPIYA-ABCCC motif derived from *H. pylori* NCTC11637. Our data showed that both of these types of CagA were degraded by autophagy induced by m1VacA (Figures 1, 2, and 3). These results suggest that CagA degradation by autophagy is not affected by differences in the EPIYA motif.

A number of studies demonstrated a link between CagA and gastric cancer development (Blaser et al., 1995; Huang et al., 2003). However, intracellular CagA was only detected in the gastric mucosa of *H. pylori*-infected patients with atrophic gastritis, and not in the gastric mucosa of patients with intestinal metaplasia or cancer (Yamazaki et al., 2003). Therefore, CagA was thought to play a causative role at a relatively early phase of gastric carcinogenesis. Our findings indicate that intracellular CagA is degraded by autophagy induced by the accumulation of intracellular ROS. Thus, even if CagA is translocated into a host cell, it does not persist for a long period. The accumulation of intracellular CagA is restricted to cells in which autophagy is suppressed. We demonstrated that intracellular CagA specifically accumulates in CD44v9-expressing human gastric cancer cells in which CagA degradation by autophagy has been suppressed by their resistance to ROS (Figure 7E). Thus, we show a direct molecular link between CagA and gastric cancer stem-like cells and suggest that the role of CagA in gastric carcinogenesis is not restricted to the early phase.

Chronic inflammation triggers the expression of CD44s (Ishimoto et al., 2010), suggesting that chronic severe inflammation after long-term *H. pylori* colonization induces CD44 expression in normal gastric epithelial cells. CD44-expressing cells have increased intracellular GSH levels, as compared to CD44-negative cells, by maintaining PPP flux and the consequent production of NADPH (Tamada et al., 2012) (Figure S5B), suggesting that CD44-positive cells are slightly resistant to oxidative stress. Conversely, CD44v9-expressing cells are more resistant to oxidative stress, compared with CD44s-expressing cells, by enhancing intracellular GSH levels through the promotion of xCT-mediated cystine uptake (Ishimoto et al., 2011) (Figure S5B). Thus, CagA specifically accumulates in CD44v9-expressing cells by escaping from the autophagy induced by ROS (Figure 7). Additionally, the mRNA expression of *lgr5*, one of the markers of stem cells besides CD44, was not detectable in the CD44- or CD44v9-expressing MKN28 cells (data not shown). Takaishi et al. (2009) reported that the expression of other potential cell-surface markers did not show any correlation with CD44-expressing gastric cancer stem cells. From these findings, we conclude that the accumulation of intracellular CagA by inhibition of autophagy is a specific character of CD44v9-expressing gastric cancer stem-like cells because of their resistance of ROS, and it does not correlate with LGR5. A variety of CD44 isoforms are generated by alternative splicing of the pre-mRNA. CD44v9 is one of the CD44 isoforms and is expressed in gastric cancer stem cells (Mayer et al., 1993). In addition, *H. pylori* infection induced CD44v9 expression, suggesting that the development of cells that accumulate CagA can be caused by *H. pylori* infection (Fan et al., 1996). CD44v9 expression, which is regulated by epithelial splicing regulatory protein 1, plays a functional role in carcinogenesis, differentiation, and metastasis (Yae et al., 2012). In addition, CagA oncogenic signals were maintained in CD44v9-expressing cancer stem-like cells in the present study.

xCT, stabilized by CD44v9, plays an important role in maintaining intracellular redox balance (Patel et al., 2004). Sulfasalazine, a potent xCT inhibitor that has been used routinely for the treatment of inflammatory bowel disease and rheumatoid arthritis, suppresses metastasis of CD44v9-expressing lung cancer and inhibits hepatocellular carcinoma cell growth (Yae et al., 2012). In the present study, sulfasalazine also inhibited the accumulation of intracellular CagA in CD44v9-expressing cells by suppressing autophagy (Figure 7D), suggesting a prophylactic effect for sulfasalazine against CagA-dependent gastric cancer development, especially by targeting cancer stemness.

EXPERIMENTAL PROCEDURES

In Vitro *H. pylori* Infection Model

Cells were incubated with s1m1VacA *H. pylori*, VacA-negative *H. pylori*, s1m2VacA *H. pylori*, and s2m2VacA *H. pylori* for 5 hr (multiplicity of infection of 50), and the cells were incubated with RPMI1640 culture medium containing 400 μg/ml kanamycin to kill extracellular bacteria with or without each inhibitor (MG132, Lact, 3MA, Wort, LY294002, nutlin-3, or sulfasalazine) or each antioxidant (acetovanillone, MnTMPyP, or NAC) for the indicated incubation period (0, 3, 15, and 24 hr). The cells were then washed three times with PBS and harvested.

Preparation of *H. pylori* Culture Supernatants

s1m1VacA, VacA-negative, s1m2VacA, and s2m2VacA *H. pylori*, normalized to an OD_{600} of 0.3, were transferred to cell culture medium (RPMI1640 medium supplemented with 10% FBS) and cultured for a further 15 hr. The supernatants were collected by centrifugation, passed through 0.22 μm filter units to remove any bacteria, and diluted with fresh medium.

Immunohistochemistry

Tissue was fixed in 4% paraformaldehyde, embedded in paraffin, and sectioned at a thickness of 4 μm. The sections were depleted of paraffin and then rehydrated in a graded series of ethanol solutions. For immunohistochemistry, the sections were washed in Tris-buffered saline with Tween-20 (TBS-T) and subjected to antigen retrieval by heating for 10 min at 105°C in Target Retrieval Solution (pH 9.0) (Dako, Tokyo). Nonspecific binding was blocked by Protein Block (Dako). The sections were incubated overnight at 4°C with primary antibody (see Supplemental Experimental Procedures). Immunoreactivity was detected using Alexa Fluor 568-conjugated goat anti-mouse IgG (Invitrogen, Carlsbad, CA), Alexa Fluor 568-conjugated goat anti-rabbit IgG (Invitrogen), and Alexa Fluor 488-conjugated goat anti-rat IgG (Invitrogen). The samples were examined using an FV10i fluorescence microscope (Olympus, Tokyo).

Electron Immunocytochemistry

CagA-expressing WT-A10 cells stimulated with 100 nM rapamycin for 24 hr were fixed with 4% paraformaldehyde and 0.1% glutaraldehyde for 80 min. The specimens were then dehydrated in a graded ethanol series and processed with a postembedding immunocytochemical technique using reduced osmium and acrylate resin. Immunogold labeling was performed by incubation with an anti-CagA goat polyclonal antibody (bK-300, 1:1000, Santa Cruz Biotechnology), followed by the addition of secondary antibodies conjugated

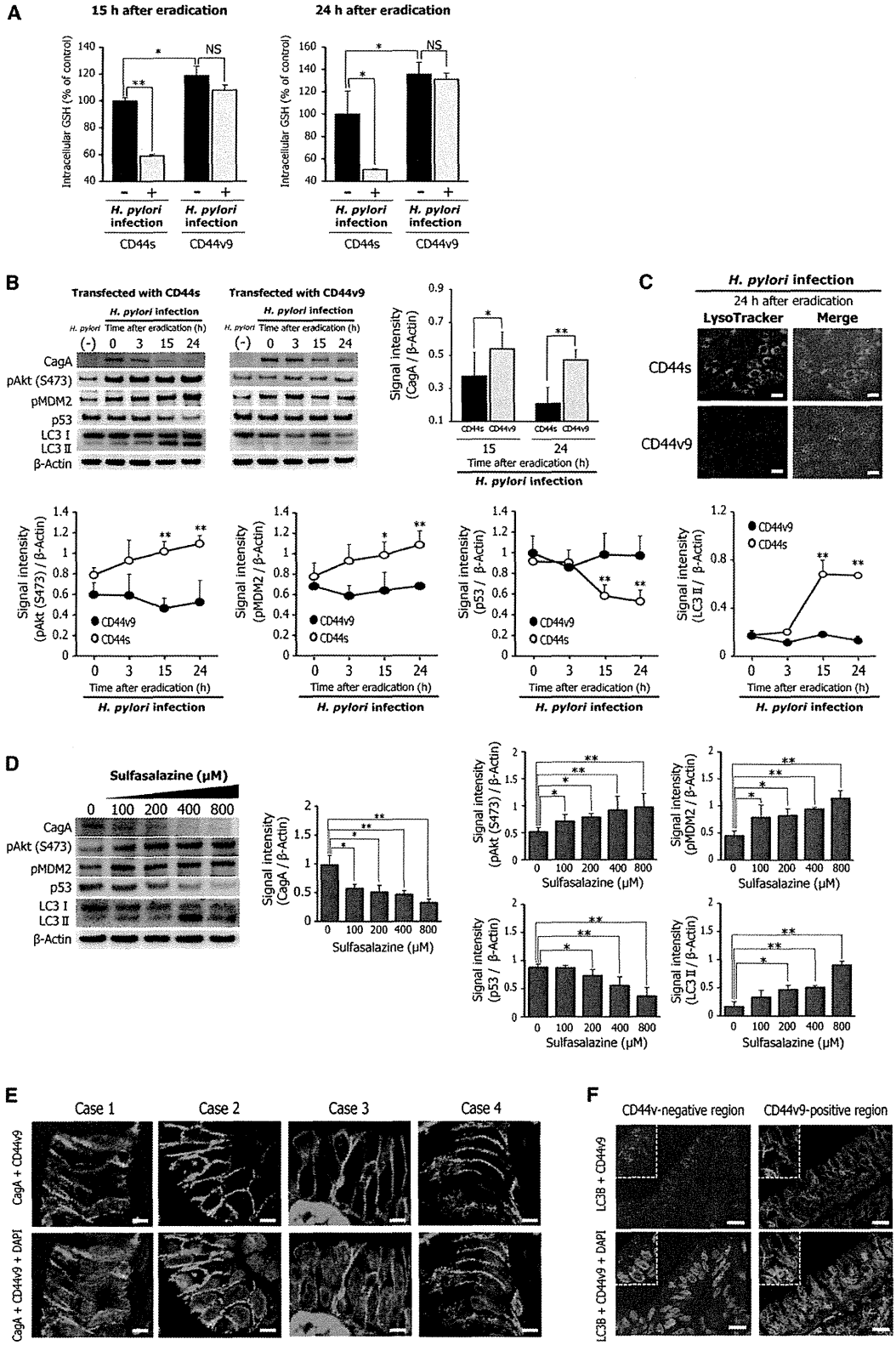

Figure 7. Accumulation of Intracellular CagA Is Detected in CD44v9-Expressing Gastric Cancer Stem-like Cells

(A) MKN28 cells were transfected with the pRC/CMV-CD44s or pRC/CMV-CD44v expression plasmid; cells infected with *H. pylori* (s1m1VacA) for 5 hr were incubated in a medium containing antibiotic for 15 and 24 hr, and intracellular GSH levels were examined. Data represent the mean ± SD of three independent assays; *p < 0.05, **p < 0.01; NS, not significant.

to 15 nm gold particles. The sections were poststained with uranyl acetate and modified Sato's lead solution and visualized using a JEM-1200EX electron microscope (JEOL, Tokyo).

Cell Vacuolation Assay

CagA expression in WT-A10 cells was induced by treatment with m1VacA or m2VacA for 24 hr, and the extent of vacuolation was determined quantitatively by measuring the uptake of neutral red.

Immunoprecipitation Assay

After s1m1VacA and s1m2VacA *H. pylori* infection for 5 hr, the cell lysates were incubated overnight with anti-LRP1 monoclonal antibody (Santa Cruz Biotechnology) at 4°C. This was followed by the addition of EZview Red Protein A Affinity Gel (Sigma) and overnight incubation. Proteins were detected using antibodies against VacA (Yahiro et al., 1999).

Fluorescence Immunocytochemistry

To detect EGFP-LC3B signals, AGS cells transfected with the EGFP-LC3B plasmid were infected with *H. pylori* for 5 hr. The cells were incubated with RPMI1640 culture medium containing 400 μg/ml kanamycin—with or without an autophagy inhibitor (3MA and Wort)—for 24 hr, fixed with 4% paraformaldehyde, and incubated with the anti-CagA antibody (AUSTRAL Biologicals). Alexa Fluor 568-conjugated goat anti-mouse IgG (Invitrogen) was used as the secondary antibody. To detect the LysoTracker signals, after *H. pylori* infection for 5 hr, the AGS cells were incubated with RPMI1640 culture medium containing 400 μg/ml kanamycin for 24 hr, and then with LysoTracker Red DND-99 (Invitrogen) for 90 min, followed by fixation with 4% paraformaldehyde. The samples were examined using an FV10i fluorescence microscope (Olympus).

Measurement of ROS

After *H. pylori* infection for 5 hr, AGS cells were incubated in RPMI1640 culture medium containing 400 μg/ml kanamycin for 15 or 24 hr. The cells were incubated with 10 μM CM-H_2DCFDA (Invitrogen) in Hanks balanced salt solution (HBSS) for 60 min at 37°C and washed three times with PBS. To label mitochondria, the cells were incubated with 10 μM MitoTracker Red FM (Invitrogen) in HBSS for 30 min. The samples were examined using an FV10i fluorescence microscope (Olympus). To quantify the intensity of DCF fluorescence, the cells were dissociated using 1 mM EDTA and subjected to flow cytometry using a Gallios Flow Cytometer (Beckman Coulter, Brea, CA) and analysis software (Summit V6.0.2.11185) (Beckman Coulter).

GSH Assay

Intracellular GSH levels were determined using a GSH-Glo Glutathione Assay Kit (Promega, Madison, WI). The cells (2×10^3 per well) were plated in 96-well plates. This assay is based on the conversion of a luciferin derivative to luciferin by glutathione S-transferase in the presence of GSH. The signal generated in a coupled reaction with firefly luciferase is proportional to the amount of GSH in the sample. The assay results were normalized using the GSH standard solution provided with the kit.

Western Blotting

Total protein (10 μg/lane) was separated on a 4%–12% NuPAGE gradient gel (Invitrogen) and transferred to a PVDF membrane (Invitrogen), which was probed with each primary antibody, followed by reprobing with an anti-actin antibody (Sigma) as the loading control. Signal detection of the immunoreactive bands was facilitated by enhanced chemiluminescence using ECL plus (GE Healthcare, Piscataway, NJ). Signal quantification was performed using the ImageJ program (National Institutes of Health).

Statistical Analysis

All values are expressed as means ± SD. The statistical significance of differences between two groups was evaluated using Student's t test. Analysis was performed using JSTAT statistical software (version 8.2). Statistical significance was accepted at $p < 0.05$, unless otherwise indicated.

Tissue Specimens

Human gastric adenocarcinoma tissue specimens were obtained from a 62-year-old female (case 1), a 68-year-old male (case 2), a 72-year-old male (case 3), a 78-year-old male (case 4), an 80-year-old female (*H. pylori*-negative patient), and a 72-year-old male (patient at 40 months after *H. pylori* eradication) who underwent endoscopic submucosal dissection at Keio University Hospital after receiving written informed consent before the procedure. Pathological diagnosis was well-differentiated adenocarcinoma according to the Japanese Gastric Cancer Association classification of gastric carcinoma (14^{th} edition). The study protocol was approved by the ethics committees of Keio University School of Medicine and registered with the UMIN Clinical Trials Registry (UMIN000001057; http://www.umin.ac.jp/ctr/). The study was performed in accordance with the principles of the Declaration of Helsinki.

SUPPLEMENTAL INFORMATION

Supplemental Information includes five figures and Supplemental Experimental Procedures and can be found with this article online at http://dx.doi.org/10.1016/j.chom.2012.10.014.

ACKNOWLEDGMENTS

The authors are grateful to Misa Kanekawa for providing general technical assistance and to Hiroshi Takase (Hanaichi Ultrastructure Research Institute) for technical assistance with electron immunocytochemistry. This work was supported by a Grant-in-Aid for Young Scientists (B) (23790156, to H.T.) and a Grant-in-Aid for Scientific Research (B) (22300169 to H.Suzuki) from the Japan Society for the Promotion of Science (JSPS), a grant from the Smoking Research Foundation (to H.Suzuki), and the Keio Gijuku Academic Development Fund (to H.Suzuki).

Received: July 20, 2012
Revised: September 22, 2012
Accepted: October 11, 2012
Published: December 12, 2012

(B) MKN28 cells were transfected with the pRC/CMV-CD44s or pRC/CMV-CD44v expression plasmid; cells infected with *H. pylori* (s1m1VacA) for 5 hr were incubated in a medium containing antibiotic for the indicated times, and intracellular CagA levels were quantified. Data represent the mean ± SD of three independent assays; *$p < 0.05$, **$p < 0.01$. Akt and MDM2 phosphorylation, p53 expression, and LC3-II formation were quantified. Data represent the mean ± SD of three independent assays; *$p < 0.05$, **$p < 0.01$, compared to each cell at 0 hr after eradication.

(C) Representative staining for LysoTracker Red DND-99 is shown. MKN28 cells were transfected with the pRC/CMV-CD44s or pRC/CMV-CD44v expression plasmid; cells infected with *H. pylori* (s1m1VacA) for 5 hr were incubated in a medium containing antibiotic for the indicated times, and the cells were stained using LysoTracker Red DND-99. Scale bar = 50 μm.

(D) MKN28 cells were transfected with the pRC/CMV-CD44v expression plasmid; cells infected with *H. pylori* ATCC700392 (s1m1VacA) for 5 hr were incubated in a medium containing antibiotic with sulfasalazine for 24 hr; and intracellular CagA, pAkt (Ser473), pMDM2, p53, and LC3-II formation were examined. Data represent the mean ± SD of three independent assays; *$p < 0.05$, **$p < 0.01$.

(E) Immunostaining of CagA and CD44v9 in human gastric adenocarcinoma. Case 1, Case 2, Case 3, and Case 4 indicate each gastric adenocarcinoma tissue specimen from the four different patients. Red staining indicates intracellular CagA and green indicates CD44v9. Nuclei (blue) were stained with DAPI. Scale bar = 20 μm.

(F) Immunostaining of LC3 and CD44v9 in human gastric adenocarcinoma. The left panel indicates a CD44v9-negative region and the right panel indicates a CD44v9-positive region. Red staining indicates LC3B-positive puncta and green indicates CD44v9. Nuclei (blue) were stained with DAPI. Scale bar = 30 μm. See also Figure S5.

REFERENCES

Atkuri, K.R., Mantovani, J.J., Herzenberg, L.A., and Herzenberg, L.A. (2007). N-Acetylcysteine—a safe antidote for cysteine/glutathione deficiency. Curr. Opin. Pharmacol. *7*, 355–359.

Basso, D., Zambon, C.F., Letley, D.P., Stranges, A., Marchet, A., Rhead, J.L., Schiavon, S., Guariso, G., Ceroti, M., Nitti, D., et al. (2008). Clinical relevance of Helicobacter pylori cagA and vacA gene polymorphisms. Gastroenterology *135*, 91–99.

Blaser, M.J., Perez-Perez, G.I., Kleanthous, H., Cover, T.L., Peek, R.M., Chyou, P.H., Stemmermann, G.N., and Nomura, A. (1995). Infection with Helicobacter pylori strains possessing cagA is associated with an increased risk of developing adenocarcinoma of the stomach. Cancer Res. *55*, 2111–2115.

Cover, T.L., and Blanke, S.R. (2005). Helicobacter pylori VacA, a paradigm for toxin multifunctionality. Nat. Rev. Microbiol. *3*, 320–332.

Dalerba, P., Dylla, S.J., Park, I.K., Liu, R., Wang, X., Cho, R.W., Hoey, T., Gurney, A., Huang, E.H., Simeone, D.M., et al. (2007). Phenotypic characterization of human colorectal cancer stem cells. Proc. Natl. Acad. Sci. USA *104*, 10158–10163.

Deretic, V., and Levine, B. (2009). Autophagy, immunity, and microbial adaptations. Cell Host Microbe *5*, 527–549.

Ding, S.Z., Minohara, Y., Fan, X.J., Wang, J., Reyes, V.E., Patel, J., Dirden-Kramer, B., Boldogh, I., Ernst, P.B., and Crowe, S.E. (2007). Helicobacter pylori infection induces oxidative stress and programmed cell death in human gastric epithelial cells. Infect. Immun. *75*, 4030–4039.

Dong-Yun, S., Yu-Ru, D., Shan-Lin, L., Ya-Dong, Z., and Lian, W. (2003). Redox stress regulates cell proliferation and apoptosis of human hepatoma through Akt protein phosphorylation. FEBS Lett. *542*, 60–64.

Fan, X., Long, A., Goggins, M., Fan, X., Keeling, P.W., and Kelleher, D. (1996). Expression of CD44 and its variants on gastric epithelial cells of patients with Helicobacter pylori colonisation. Gut *38*, 507–512.

Hatakeyama, M. (2004). Oncogenic mechanisms of the Helicobacter pylori CagA protein. Nat. Rev. Cancer *4*, 688–694.

Huang, J.Q., Zheng, G.F., Sumanac, K., Irvine, E.J., and Hunt, R.H. (2003). Meta-analysis of the relationship between cagA seropositivity and gastric cancer. Gastroenterology *125*, 1636–1644.

Huang, J., Canadien, V., Lam, G.Y., Steinberg, B.E., Dinauer, M.C., Magalhaes, M.A., Glogauer, M., Grinstein, S., and Brumell, J.H. (2009). Activation of antibacterial autophagy by NADPH oxidases. Proc. Natl. Acad. Sci. USA *106*, 6226–6231.

Ishikawa, S., Ohta, T., and Hatakeyama, M. (2009). Stability of Helicobacter pylori CagA oncoprotein in human gastric epithelial cells. FEBS Lett. *583*, 2414–2418.

Ishimoto, T., Oshima, H., Oshima, M., Kai, K., Torii, R., Masuko, T., Baba, H., Saya, H., and Nagano, O. (2010). CD44+ slow-cycling tumor cell expansion is triggered by cooperative actions of Wnt and prostaglandin E2 in gastric tumorigenesis. Cancer Sci. *101*, 673–678.

Ishimoto, T., Nagano, O., Yae, T., Tamada, M., Motohara, T., Oshima, H., Oshima, M., Ikeda, T., Asaba, R., Yagi, H., et al. (2011). CD44 variant regulates redox status in cancer cells by stabilizing the xCT subunit of system xc(-) and thereby promotes tumor growth. Cancer Cell *19*, 387–400.

Marshall, D.G., Hynes, S.O., Coleman, D.C., O'Morain, C.A., Smyth, C.J., and Moran, A.P. (1999). Lack of a relationship between Lewis antigen expression and cagA, CagA, vacA and VacA status of Irish Helicobacter pylori isolates. FEMS Immunol. Med. Microbiol. *24*, 79–90.

Mayer, B., Jauch, K.W., Günthert, U., Figdor, C.G., Schildberg, F.W., Funke, I., and Johnson, J.P. (1993). De-novo expression of CD44 and survival in gastric cancer. Lancet *342*, 1019–1022.

Miehlke, S., Kirsch, C., Agha-Amiri, K., Günther, T., Lehn, N., Malfertheiner, P., Stolte, M., Ehninger, G., and Bayerdörffer, E. (2000). The Helicobacter pylori vacA s1, m1 genotype and cagA is associated with gastric carcinoma in Germany. Int. J. Cancer *87*, 322–327.

Ogawara, Y., Kishishita, S., Obata, T., Isazawa, Y., Suzuki, T., Tanaka, K., Masuyama, N., and Gotoh, Y. (2002). Akt enhances Mdm2-mediated ubiquitination and degradation of p53. J. Biol. Chem. *277*, 21843–21850.

Ohnishi, N., Yuasa, H., Tanaka, S., Sawa, H., Miura, M., Matsui, A., Higashi, H., Musashi, M., Iwabuchi, K., Suzuki, M., et al. (2008). Transgenic expression of Helicobacter pylori CagA induces gastrointestinal and hematopoietic neoplasms in mouse. Proc. Natl. Acad. Sci. USA *105*, 1003–1008.

Patel, S.A., Warren, B.A., Rhoderick, J.F., and Bridges, R.J. (2004). Differentiation of substrate and non-substrate inhibitors of transport system xc(-): an obligate exchanger of L-glutamate and L-cystine. Neuropharmacology *46*, 273–284.

Raju, D., Hussey, S., Ang, M., Terebiznik, M.R., Sibony, M., Galindo-Mata, E., Gupta, V., Blanke, S.R., Delgado, A., Romero-Gallo, J., et al. (2012). Vacuolating cytotoxin and variants in Atg16L1 that disrupt autophagy promote Helicobacter pylori infection in humans. Gastroenterology *142*, 1160–1171.

Saito, Y., Murata-Kamiya, N., Hirayama, T., Ohba, Y., and Hatakeyama, M. (2010). Conversion of Helicobacter pylori CagA from senescence inducer to oncogenic driver through polarity-dependent regulation of p21. J. Exp. Med. *207*, 2157–2174.

Scherz-Shouval, R., and Elazar, Z. (2007). ROS, mitochondria and the regulation of autophagy. Trends Cell Biol. *17*, 422–427.

Suzuki, H., Suematsu, M., Ishii, H., Kato, S., Miki, H., Mori, M., Ishimura, Y., Nishino, T., and Tsuchiya, M. (1994). Prostaglandin E1 abrogates early reductive stress and zone-specific paradoxical oxidative injury in hypoperfused rat liver. J. Clin. Invest. *93*, 155–164.

Suzuki, H., Iwasaki, E., and Hibi, T. (2009). Helicobacter pylori and gastric cancer. Gastric Cancer *12*, 79–87.

Takaishi, S., Okumura, T., Tu, S., Wang, S.S., Shibata, W., Vigneshwaran, R., Gordon, S.A., Shimada, Y., and Wang, T.C. (2009). Identification of gastric cancer stem cells using the cell surface marker CD44. Stem Cells *27*, 1006–1020.

Tamada, M., Nagano, O., Tateyama, S., Ohmura, M., Yae, T., Ishimoto, T., Sugihara, E., Onishi, N., Yamamoto, T., Yanagawa, H., et al. (2012). Modulation of glucose metabolism by CD44 contributes to antioxidant status and drug resistance in cancer cells. Cancer Res. *72*, 1438–1448.

Terebiznik, M.R., Raju, D., Vázquez, C.L., Torbricki, K., Kulkarni, R., Blanke, S.R., Yoshimori, T., Colombo, M.I., and Jones, N.L. (2009). Effect of Helicobacter pylori's vacuolating cytotoxin on the autophagy pathway in gastric epithelial cells. Autophagy *5*, 370–379.

Uemura, N., Okamoto, S., Yamamoto, S., Matsumura, N., Yamaguchi, S., Yamakido, M., Taniyama, K., Sasaki, N., and Schlemper, R.J. (2001). Helicobacter pylori infection and the development of gastric cancer. N. Engl. J. Med. *345*, 784–789.

Wang, H.J., Kuo, C.H., Yeh, A.A., Chang, P.C., and Wang, W.C. (1998). Vacuolating toxin production in clinical isolates of Helicobacter pylori with different vacA genotypes. J. Infect. Dis. *178*, 207–212.

Wei, J., Nagy, T.A., Vilgelm, A., Zaika, E., Ogden, S.R., Romero-Gallo, J., Piazuelo, M.B., Correa, P., Washington, M.K., El-Rifai, W., et al. (2010). Regulation of p53 tumor suppressor by Helicobacter pylori in gastric epithelial cells. Gastroenterology *139*, 1333–1343.

Yae, T., Tsuchihashi, K., Ishimoto, T., Motohara, T., Yoshikawa, M., Yoshida, G.J., Wada, T., Masuko, T., Mogushi, K., Tanaka, H., et al. (2012). Alternative splicing of CD44 mRNA by ESRP1 enhances lung colonization of metastatic cancer cell. Nat Commun. *3*, 883.

Yahiro, K., Niidome, T., Kimura, M., Hatakeyama, T., Aoyagi, H., Kurazono, H., Imagawa, K., Wada, A., Moss, J., and Hirayama, T. (1999). Activation of Helicobacter pylori VacA toxin by alkaline or acid conditions increases its binding to a 250-kDa receptor protein-tyrosine phosphatase beta. J. Biol. Chem. *274*, 36693–36699.

Yahiro, K., Satoh, M., Nakano, M., Hisatsune, J., Isomoto, H., Sap, J., Suzuki, H., Nomura, F., Noda, M., Moss, J., and Hirayama, T. (2012). Low-density lipoprotein receptor-related protein-1 (LRP1) mediates autophagy and apoptosis caused by Helicobacter pylori VacA. J. Biol. Chem. *287*, 31104–31115.

Yamaoka, Y., Kodama, T., Kita, M., Imanishi, J., Kashima, K., and Graham, D.Y. (1998). Relationship of vacA genotypes of Helicobacter pylori to cagA status, cytotoxin production, and clinical outcome. Helicobacter *3*, 241–253.

Yamazaki, S., Yamakawa, A., Ito, Y., Ohtani, M., Higashi, H., Hatakeyama, M., and Azuma, T. (2003). The CagA protein of Helicobacter pylori is translocated into epithelial cells and binds to SHP-2 in human gastric mucosa. J. Infect. Dis. *187*, 334–337.

Yokoyama, K., Higashi, H., Ishikawa, S., Fujii, Y., Kondo, S., Kato, H., Azuma, T., Wada, A., Hirayama, T., Aburatani, H., and Hatakeyama, M. (2005). Functional antagonism between Helicobacter pylori CagA and vacuolating toxin VacA in control of the NFAT signaling pathway in gastric epithelial cells. Proc. Natl. Acad. Sci. USA *102*, 9661–9666.

Zhou, B.P., Liao, Y., Xia, W., Zou, Y., Spohn, B., and Hung, M.C. (2001). HER-2/neu induces p53 ubiquitination via Akt-mediated MDM2 phosphorylation. Nat. Cell Biol. *3*, 973–982.

CDX1 confers intestinal phenotype on gastric epithelial cells via induction of stemness-associated reprogramming factors SALL4 and KLF5

Yumiko Fujii[a,b], Kyoko Yoshihashi[a], Hidekazu Suzuki[c], Shuichi Tsutsumi[d], Hiroyuki Mutoh[e], Shin Maeda[f], Yukinori Yamagata[g], Yasuyuki Seto[g], Hiroyuki Aburatani[d], and Masanori Hatakeyama[a,1]

[a]Division of Microbiology, Graduate School of Medicine, The University of Tokyo, Tokyo 113-0033, Japan; [b]Division of Chemistry, Graduate School of Science, Hokkaido University, Sapporo 060-0810, Japan; [c]Division of Gastroenterology and Hepatology, Department of Internal Medicine, Keio University School of Medicine, Tokyo 160-8582, Japan; [d]Genome Science Division, Research Center for Advanced Science and Technology, The University of Tokyo, Tokyo 153-8904, Japan; [e]Division of Gastroenterology, Department of Medicine, Jichi Medical University, Tochigi 329-0498, Japan; [f]Department of Gastroenterology, Yokohama City University Graduate School of Medicine, Yokohama 236-0004, Japan; and [g]Department of Gastrointestinal Surgery, Graduate School of Medicine, The University of Tokyo, Tokyo 113-8655, Japan

Edited[†] by Tadatsugu Taniguchi, The University of Tokyo, Tokyo, Japan, and approved October 4, 2012 (received for review May 22, 2012)

Intestinal metaplasia of the stomach, a mucosal change characterized by the conversion of gastric epithelium into an intestinal phenotype, is a precancerous lesion from which intestinal-type gastric adenocarcinoma arises. Chronic infection with *Helicobacter pylori* is a major cause of gastric intestinal metaplasia, and aberrant induction by *H. pylori* of the intestine-specific caudal-related homeobox (CDX) transcription factors, CDX1 and CDX2, plays a key role in this metaplastic change. As such, a critical issue arises as to how these factors govern the cell- and tissue-type switching. In this study, we explored genes directly activated by CDX1 in gastric epithelial cells and identified stemness-associated reprogramming factors *SALL4* and *KLF5*. Indeed, *SALL4* and *KLF5* were aberrantly expressed in the CDX1$^+$ intestinal metaplasia of the stomach in both humans and mice. In cultured gastric epithelial cells, sustained expression of CDX1 gave rise to the induction of early intestinal-stemness markers, followed by the expression of intestinal-differentiation markers. Furthermore, the induction of these markers was suppressed by inhibiting either SALL4 or KLF5 expression, indicating that CDX1-induced SALL4 and KLF5 converted gastric epithelial cells into tissue stem-like progenitor cells, which then transdifferentiated into intestinal epithelial cells. Our study places the stemness-related reprogramming factors as critical components of CDX1-directed transcriptional circuitries that promote intestinal metaplasia. Requirement of a transit through dedifferentiated stem/progenitor-like cells, which share properties in common with cancer stem cells, may underlie predisposition of intestinal metaplasia to neoplastic transformation.

CagA | Wnt | β-catenin

Metaplasia is a histological change from one tissue type to another, which is associated with conversion of its respective cell types to the corresponding ones. Metaplastic changes can occur either in a physiological process or a pathological condition, the latter of which predisposes cells to undergo neoplastic transformation via a metaplasia–dysplasia–carcinoma sequence. Intestinal metaplasia, a pathological change of non-intestinal epithelium into an intestinal-like mucosa, is most frequently found in the stomach and esophagus (1, 2). *Helicobacter pylori*-induced chronic gastritis is a major cause of gastric intestinal metaplasia, from which intestinal-type adenocarcinoma arises (3). Likewise, replacement of the esophageal squamous epithelium by intestinal epithelium known as Barrett's esophagus substantially increases the risk of esophageal adenocarcinoma (2).

The *Drosophila* homeobox gene *caudal* plays a critical role in development of the posterior embryo (4). *Caudal* has three homologs in vertebrates (*CDX1*, *CDX2*, and *CDX4* in humans; *Cdx1*, *Cdx2*, and *Cdx4* in mice; and *CdxA*, *CdxB*, and *CdxC* in chickens) (5, 6). These genes encode Caudal-related homeobox transcription factors (hereafter denoted as CDX family proteins), which play unique roles in axial patterning and gut development by regulating specific genes through binding to an A/T-rich responsive element. The consensus binding sequence for these CDX family proteins is (A/C)TTTAT(A/G), in which TTTAT acts as a conserved core motif (4, 5). In mammals, CDX family members, especially CDX1 and CDX2, are critically involved in development and maintenance of the intestine (6). Indeed, both CDX1/Cdx1 and CDX2/Cdx2 are expressed in the epithelium of the large and small intestines but not in the epithelium of the stomach or esophagus. They are, however, aberrantly expressed in the intestinal metaplastic lesion of the stomach as well as in Barrett's esophagus (6). *CDX1* is transactivated by several distinct signaling mechanisms such as Wnt/β-catenin signal and retinoic acid signal (7). We previously reported that *H. pylori* CagA, which is delivered into gastric epithelial cells via bacterial type IV secretion, aberrantly stimulates β-catenin signaling and thereby induces Wnt target genes including *CDX1* (8). This observation suggested that CagA-mediated Wnt/β-catenin deregulation plays an important role in the ectopic expression of CDX1 in the stomach infected with *H. pylori*.

Transgenic expression of Cdx1 or Cdx2 in mouse stomach causes intestinal metaplasia (9, 10), indicating a causal and redundant role of ectopically expressed CDX1 and CDX2 in the metaplastic change. Because metaplasia is defined as a switching from one tissue to another, the process may be initiated through changes in cell differentiation status so as to acquire some sort of cell/tissue stemness or multipotency. However, little is known about CDX-governed transcriptional circuitries that give rise to intestinal metaplasia of the stomach. In this work, we investigated genes directly activated by CDX1 in gastric epithelial cells by combining expression microarray and chromatin immunoprecipitation (ChIP)-chip analyses and identified transcription factors, *SALL4* and *KLF5*, both of which are involved in lineage reprogramming and stemness acquisition. We show that CDX1-mediated induction of *SALL4* and *KLF5* plays an important role in transdifferentiation of gastric epithelial cells into an intestinal phenotype, which underlies intestinal metaplasia of the stomach.

Author contributions: Y.F. and M.H. designed research; Y.F., K.Y., and M.H. performed research; H.S., S.T., H.M., S.M., Y.Y., Y.S., and H.A. contributed new reagents/analytic tools; Y.F., K.Y., S.T., H.A., and M.H. analyzed data; and Y.F. and M.H. wrote the paper.

The authors declare no conflict of interest.

[†]This Direct Submission article had a prearranged editor.

Data deposition: The data reported in this paper have been deposited in the Gene Expression Omnibus (GEO) database, www.ncbi.nlm.nih.gov/geo (accession no. GSE35369).

See Commentary on page 20173.

[1]To whom correspondence should be addressed. E-mail: mhata@m.u-tokyo.ac.jp.

This article contains supporting information online at www.pnas.org/lookup/suppl/doi:10.1073/pnas.1208651109/-/DCSupplemental.

Results

Genes Affected by Ectopic CDX1 Expression in Gastric Epithelial Cells. To investigate genes targeted by ectopically expressed CDX1, we established several transfectant clones that inducibly express Flag-tagged CDX1 from MNK28 human gastric epithelial cells using a tetracycline-regulated Tet-Off system (Fig. 1 *A* and *B* and Fig. S1*A*). Among these, MKN28-A2 cells, which showed the highest expression upon depletion of doxycycline (Dox), a water-soluble tetracycline analog, were subjected to expression microarray analysis and ChIP-chip analysis. First, we compared mRNA expression profiles of MKN28-A2 cells cultured in the presence (CDX1 induction −) or absence (CDX1 induction +) of Dox for 24 h through genome-wide expression microarray analysis and identified 958 genes that showed increases in transcript levels of more than twofold after CDX1 induction and 260 genes whose expression levels were decreased to less than half by CDX1 expression (Fig. 1*C*). Because the removal of Dox had little impact on the mRNA expression profile in parental MKN28 (*tet-off*) cells (Dataset S1), genes selected in Fig. 1*C* were due to specific induction of CDX1. We next carried out ChIP-chip analysis using a human promoter array. CDX1 mostly bound to the promoter regions that are localized substantially upstream of the transcription start sites (TSSs) of genes (Fig. S1*B*). The results of ChIP-chip analysis revealed 1,997 genes to which CDX1 binds at the regulatory regions (Fig. 1*C*). These identified genes contained known CDX1-target genes (Fig. S1*C*). By combining data obtained from expression microarray and ChIP-chip analyses, we selected 166 genes that should include genes specifically up-regulated by CDX1 (Fig. 1*C* and Dataset S2). Unlike a bacterial restriction endonuclease, which strictly recognizes a unique nucleotide sequence, a mammalian transcription factor binds to a range of related sequences (11). Indeed, in the CDX consensus (A/C)TTTAT(A/G), positions 1 and 7 are less stringent compared with the core motif TTTAT (positions 2–6) (5). Given this, we investigated sequences that were enriched in the upstream regions of CDX1-induced genes and found that TTTATT was overrepresented in these regions (Fig. S1*D*). This result reinforced the importance of the TTTAT core motif for specific DNA binding of CDX family proteins. The result also raised the possibility that, whereas CDX1 can variably interact with a number of sequences related to the CDX consensus (A/C)TTTAT(A/G), it preferentially binds to TTTATT. The slight difference between TTTATT and the CDX consensus may allow CDX1 to regulate genes in a manner that is quantitatively and/or qualitatively different from that by which genes are regulated by other CDX members.

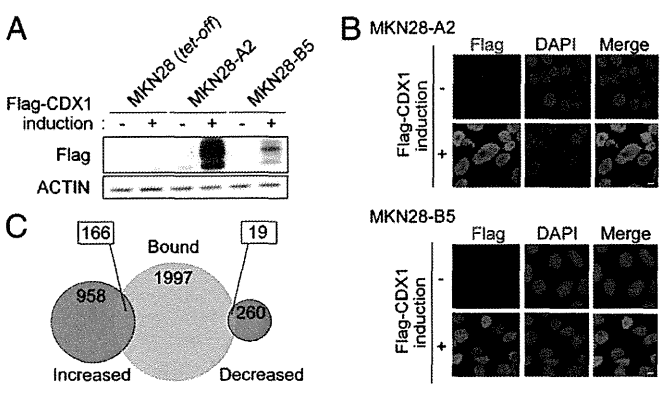

Fig. 1. Transcriptional targets of CDX1. (*A*) Lysates prepared from MKN28 (*tet-off*) cells and the transfectant clones, MKN28-A2 and MKN28-B5 cells, were subjected to immunoblotting with the respective antibodies. Flag-tagged CDX1 was induced by Dox depletion. (*B*) Anti-Flag immunostaining of MKN28-A2 and MKN28-B5 cells with or without Flag-CDX1 induction. Nuclei were visualized by DAPI. (Scale bars, 10 μm.) (*C*) Venn diagram showing the overlap between genes to which CDX1 bound and those of which mRNA levels were altered by CDX1 expression.

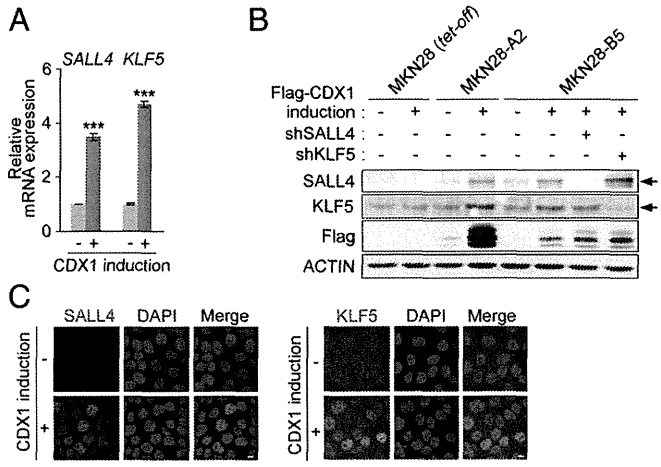

Fig. 2. Induction of SALL4 and KLF5 by CDX1. (*A*) *SALL4* and *KLF5* mRNA levels in MKN28-A2 cells with or without CDX1 induction for 24 h were determined by RT-qPCR. Error bars, ± SD; $n = 3$. (*B*) Cells transfected with an expression vector for a SALL4- or KLF5-specific short hairpin RNA (shRNA), pSUPER-shSALL4/1 or pSUPER-shKLF5/1, were induced to express Flag-CDX1 by Dox depletion for 24 h. Lysates prepared were immunoblotted with the respective antibodies. Arrows indicate the positions of SALL4 and KLF5. (*C*) MKN28-B5 cells were immunostained with the respective antibodies. Flag-CDX1 was induced for 48 h. (Scale bars, 10 μm.)

Transactivation of Reprogramming Factors by Ectopic CDX1. We hypothesized that CDX1 induces stemness-regulating reprogramming factors in gastric epithelial cells that revert cell-differentiation status so that the cells acquire intestinal stem/progenitor-like properties. With this idea, we investigated whether the identified CDX1-target genes included genes that could confer multipotency upon differentiated somatic cells and we found *Sal-like 4* (*SALL4* in humans and *Sall4* in mice), a gene encoding the SALL4/Sall4 transcription factor that is essential for maintaining stemness in embryonic stem (ES) cells (Dataset S2) (12, 13). Of note, *Sall4* is not expressed in the adult gastrointestinal tract under physiological conditions (14). The identified CDX1-target genes also included *Krüppel-like factor 5* (*KLF5* in humans and *Klf5* in mice), which encodes the KLF5/Klf5 transcription factor (Dataset S2). Klf5 is capable of replacing Klf4 in generating inducible pluripotent stem (iPS) cells, indicating its role in the acquisition of stemness (15). Whereas *Klf5* is predominantly expressed in the small intestine and colon, a small amount of the *Klf5* transcript is also detectable in the stomach (16). A reverse–transcription quantitative PCR (RT-qPCR) analysis revealed that both *SALL4* and *KLF5* mRNAs were induced in MKN28-A2 cells upon ectopic expression of CDX1 (Fig. 2*A*). Induction of endogenous SALL4 and KLF5 by CDX1 was also demonstrated through immunostaining or immunoblotting (Fig. 2 *B* and *C*). ChIP-chip analysis revealed that CDX1 binds to the sequence between −2083 and −737 of the *SALL4* promoter, which contains two CDX-binding TTTAT core motifs conserved between the human and mouse sequences (Fig. 3*A*, *Left* and Fig. S2). A luciferase reporter assay using a series of deletion mutants of the *SALL4* promoter showed that the sequence between −1305 and −938, which contains a single putative CDX-binding sequence, was involved in induction of *SALL4* by CDX1 (Fig. 3*B*, *Left*). A further deletion of the *SALL4* regulatory region from −938 to −642 slightly but significantly restored the reporter activity. This observation was reproduced in the nontransformed human gastric epithelial cell line GES-1 (Fig. S3), indicating the presence of a *cis*-acting repressor element between −938 and −642. The results of ChIP-chip analysis also showed that CDX1 binds to

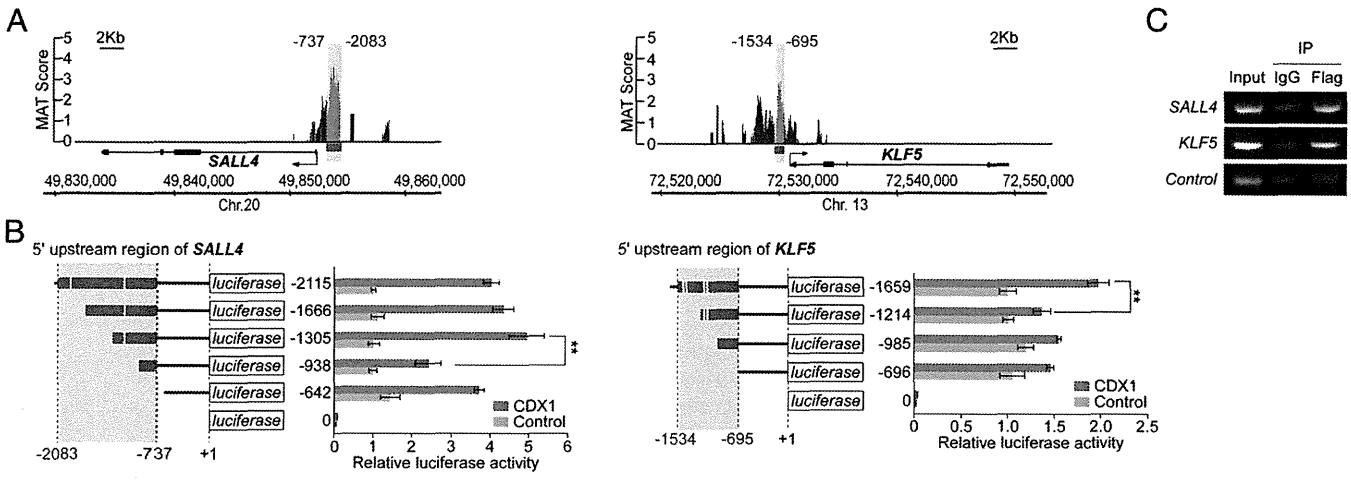

Fig. 3. Transactivation of *SALL4* and *KLF5* by CDX1. (*A*) ChIP-chip signals at the *SALL4* or *KLF5* loci. Red lines represent CDX1-binding regions. (*B*) MKN28 cells transfected with the indicated reporter plasmids together with a CDX1 or control vector were subjected to luciferase reporter assay. Schematic diagrams represent *SALL4* (*Left*) or *KLF5* (*Right*) upstream regions. Numbers indicate the distance from the TSS. Red lines indicate the CDX1-binding regions identified in *A* and yellow boxes represent putative CDX1-binding sites containing the TTTAT core motif. Error bars, ± SD; $n = 3$. (*C*) ChIP-PCR analysis for Flag-CDX1 occupancies of the *SALL4* and *KLF5* upstream regions in CDX1-induced MKN28-A2 cells.

the sequence between −1534 and −695 of the *KLF5* promoter (Fig. 3*A*, *Right* and Fig. S2), which contains four CDX1-binding core motifs conserved between the human and mouse sequences. To further elucidate the enhancer element that is used for CDX1-dependent transactivation of *KLF5*, a luciferase reporter assay was carried out using a series of deletion mutants for the *KLF5* promoter region. The results of the experiment revealed that CDX1 transactivates *KLF5* via the sequence between −1659 and −1214 that contains two putative CDX1-binding sites (Fig. 3*B*, *Right*). In both *SALL4* and *KLF5* cases, reduction in luciferase activity by deletion of the putative CDX1-binding sites was not robust. In eukaryotes, however, rarely does a single transcription factor govern transcription of the target gene. Instead, different combinations of ubiquitous and cell-type–specific transcription factors act together by binding to the respective binding sites, with each one having a differential functional contribution (17). Hence, despite its partial promoter stimulation, CDX1 may play a pivotal role in passing a certain threshold of the promoter activation that is required for ectopic expression of *SALL4* and *KLF5*. By ChIP experiment, specific binding of CDX1 to the upstream regulatory regions of *SALL4* and *KLF5* were confirmed (Fig. 3*C*). Based on these observations, we concluded that *SALL4* and *KLF5* are direct transcriptional targets of CDX1.

To generalize the above-described observations, we transiently transfected a Flag-tagged CDX1 vector into AGS and GES-1 human gastric epithelial cells. The results of luciferase reporter assays confirmed that CDX1 transactivates *SALL4* and *KLF5* in both cells (Fig. 4*A*). A ChIP experiment revealed that CDX1 bound to the upstream regions of *SALL4* and *KLF5* genes (Fig. 4*B*). Induction of SALL4 and KLF5 proteins by ectopic expression of CDX1 was also demonstrated in AGS and GES-1 cells (Fig. 4*C*).

To investigate the pathophysiological relevance for induction of these reprogramming factors in intestinal metaplasia, expression of *Sall4* and *Klf5* was investigated in the stomach of Cdx1-transgenic mice using RT-qPCR and found that both of the mRNAs were detectable in the intestinal metaplastic lesions of the mouse stomach (Fig. 4*D*). The expression of *SALL4* and *KLF5* was also examined in intestinal metaplasia of the human stomach by semiquantitative RT-PCR (Fig. 4*E*). In control RNAs obtained from gastric mucosa without intestinal metaplasia

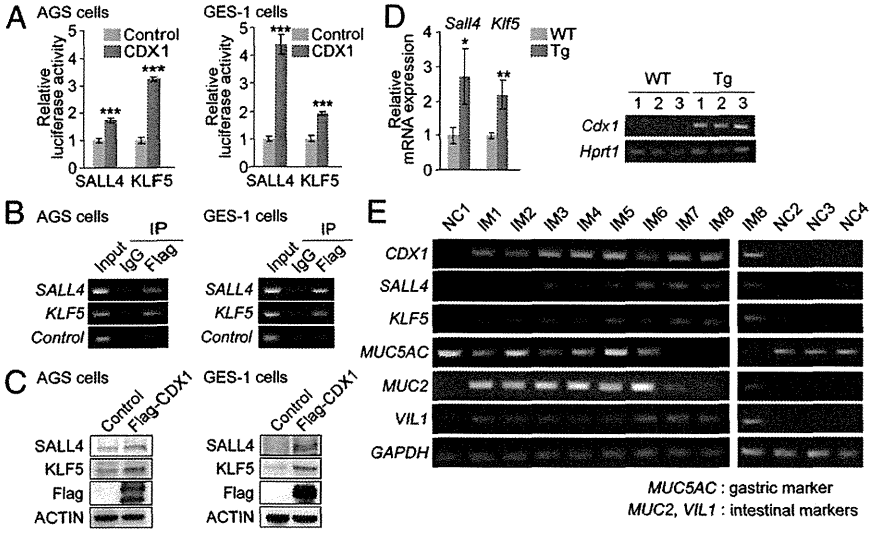

Fig. 4. Aberrant expression of *SALL4* and *KLF5* in intestinal metaplasia. (*A*) Cells transfected with pGL3-*SALL4*(−1305) or pGL3-*KLF5*(−1659) reporter plasmid together with a CDX1 or control vector were subjected to luciferase reporter assay. Error bars, ± SD; $n = 3$. (*B*) ChIP-PCR analysis for Flag-CDX1 occupancies of the *SALL4* and *KLF5* upstream regions in cells transiently transfected with a Flag-CDX1 vector. (*C*) Induction of SALL4 and KLF5 in cells transiently transfected with a Flag-CDX1 vector. (*D*) Levels of *SALL4* and *KLF5* mRNAs in the stomach of wild-type (WT) and Cdx1-transgenic (Tg) mice were determined by RT-qPCR. Error bars, ± SD; $n = 3$ (*Left*). Transgenic expression of *Cdx1* in the stomach of Cdx1-Tg mice was confirmed by RT-PCR (*Right*). (*E*) Expression of the indicated mRNAs in human stomachs with (IM1–IM8) or without (NC1–NC4) intestinal metaplasia was determined by semiquantitative RT-PCR.

[normal control (NC1-NC4)], *CDX1*, *SALL4*, or *KLF5* was hardly detectable. In contrast, in samples in which *CDX1* was expressed [intestinal metaplasia (IM1-IM8)], *KLF5* was also detectable and the level of *KLF5* expression was in proportion to the level of CDX1 expression. *SALL4* was also detected in samples IM3–IM8. However, it was only weakly expressed in samples IM1 and IM2, in which the expression levels of CDX1 were less than those in samples IM3–IM8. Induction of *SALL4* may therefore require a higher level of CDX1 expression than that required for *KLF5* induction. In samples IM1–IM6, both gastric mucin (*MUC5AC*) and intestinal mucin (*MUC2*) were detected, indicating that these samples contained both intestinal metaplastic lesions and normal gastric mucosa. In samples IM7 and IM8, the level of mucin expression, either intestinal or gastric type, was low, whereas that of *Villin1* (*VIL1*) was high. Although *VIL1* is known as an enterocyte marker, it is also expressed in gastrointestinal stem/progenitor cells (18). Accordingly, samples IM7 and IM8 may have been derived from lesions that persisted in a less-differentiated state rather than having undergone transdifferentiation. These observations provided in vivo evidence that *KLF5* and *SALL4* were aberrantly expressed in intestinal metaplasia of the stomach in both humans and mice.

Induction of Intestinal Stem/Progenitor Markers by CDX1. Through microarray analysis, the genes activated by CDX1 in gastric epithelial cells also included genes expressed in intestinal progenitor cells such as *GATA binding protein 6* (*GATA6*) and *follistatin* (*FST*). GATA6 is expressed in the intestinal crypt and involved in proliferation of immature cells (19). Likewise, FST, an antagonist of TGF-β superfamily proteins, is expressed in undifferentiated intestinal epithelial cells (20). RT-qPCR analysis exhibited one order-of-magnitude increase in the level of *GATA6* or *FST* upon ectopic CDX1 expression in gastric epithelial cells (Fig. 5*A*).

Recent studies have demonstrated that intestinal stem cells are characterized by the expression of intestinal-stemness markers (21). Microarray analysis demonstrated that one of the genes most robustly induced by ectopic CDX1 in gastric epithelial cells was *leucine-rich repeat containing G protein-coupled receptor 5* (*LGR5*), an intestinal-stemness marker (Table S1). Ectopic CDX1 also gave rise to the expression of other intestinal-stemness markers, such as *BMI1 polycomb ring finger oncogene* (*BMI1*) (Table S1). RT-qPCR analysis confirmed increased expression of *LGR5* and *BMI1* upon CDX1 expression in MKN28-A2 cells (Fig. 5*B*). Although highly reproducible and statistically significant, induction of *BMI1* mRNA by CDX1 was relatively weak. This was most probably due to the higher level of CDX1 required for activation of *BMI1* than that required for activation of *LGR5*. From these observations, we concluded that aberrantly expressed CDX1 endowed gastric epithelial cells with an intestinal stem/progenitor-like phenotype.

Up-Regulation of Intestinal-Differentiation Markers by Sustained CDX1 Expression in Gastric Epithelial Cells. Intestinal metaplasia comprises variably differentiated intestinal epithelial cell lineages such as absorptive enterocytes, goblet cells, enteroendocrine cells, and Paneth cells in nonintestinal epithelium (1, 2). Transgenic expression of Cdx1 has been reported to induce all of those epithelial cell lineages in the mouse stomach (9). Consistently, microarray analysis demonstrated that ectopic expression of CDX1 in gastric epithelial cells induces *sucrase-isomaltase* (*SI*) and *membrane metallo-endopeptidase* (*MME*), which are physiologically expressed in absorptive enterocytes of the small intestine. *Vasoactive intestinal peptide* (*VIP*), a gastrointestinal hormone secreted from enteroendocrine cells in the small intestine, was also induced upon CDX1 expression in gastric epithelial cells. RT-qPCR experiments confirmed up-regulation of these intestine-differentiation markers in gastric epithelial cells by CDX1 (Fig. 5*C*). The expression levels of these intestinal-differentiation markers increased progressively upon sustained

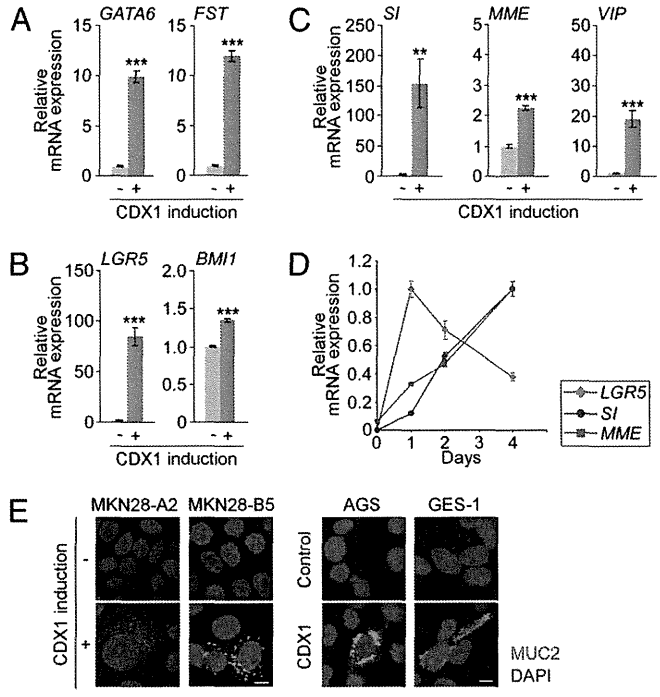

Fig. 5. Induction of intestinal markers by CDX1 in gastric epithelial cells. (*A–C*) Levels for intestinal-progenitor markers (*A*), intestinal-stemness markers (*B*), and intestinal-differentiation markers (*C*) in MKN28-A2 cells before and after induction of CDX1 for 24 h were determined by RT-qPCR. Error bars, ± SD; n = 3. (*D*) Kinetic changes in the expression of the respective genes following induction of CDX1 in MKN28-A2 cells were determined by RT-qPCR. Error bars, ± SD; n = 3. (*E*) Anti-MUC2 immunostaining of cells inducibly expressing Flag-CDX1 (*Left*) or transiently transfected with a Flag-CDX1 vector (*Right*) for 4 d. (Scale bars, 10 μm.)

CDX1 expression, whereas that of the intestinal-stemness marker reached a peak within 24 h after CDX1 induction (Fig. 5*D*). *MUC2*, a goblet cell marker, was not detected within 24 h after CDX1 induction. However, in all gastric epithelial cells examined (MKN28, AGS, and GES-1), a fraction of cells became MUC2$^+$ after prolonged exposure (~4 d) to CDX1 (Fig. 5*E*). The Paneth cell and the enteroendocrine cell markers were negative following sustained CDX1 expression in cultured gastric cells (Fig. S4). Thus, CDX1 on its own may support differentiation into absorptive enterocytes and goblet cells in a cell autonomous fashion. Development of other types of intestinal epithelial cells might require non–cell-autonomous signals in addition to CDX1. Also notably, most of these intestinal-differentiation markers were not likely to be directly transactivated by ectopic CDX1 in gastric epithelial cells (Dataset S2), suggesting that they were induced via de novo formation of CDX1-governed transcriptional circuitries that promote intestinal differentiation.

Requirement of SALL4 and KLF5 in CDX1-Mediated Intestinal Transdifferentiation. To investigate the role of SALL4 and/or KLF5 induction in the transdifferentiation of gastric epithelial cells by ectopic CDX1, we established two independent CDX1-inducible MKN28 cell lines, A2-KD/SK and B5-KD/SK, in which expression of both SALL4 and KLF5 was suppressed by stable expression of specific shRNA vectors (Fig. 6 *A* and *B*, *Left*). MKN28 cells expressing a luciferase-specific shRNA (A2-KD/C and B5-KD/C) were also established and were used as a control. Increased CDX1 expression or decreased SALL4/KLF5 expression had no relevance to the expression levels of transcription factors such as NF-κB p65/v-rel reticuloendotheliosis viral oncogene homolog A (RelA) and specificity protein 1 (Sp1), which may not be regulated by CDX1, SALL4, or KLF5 (Fig. S5).

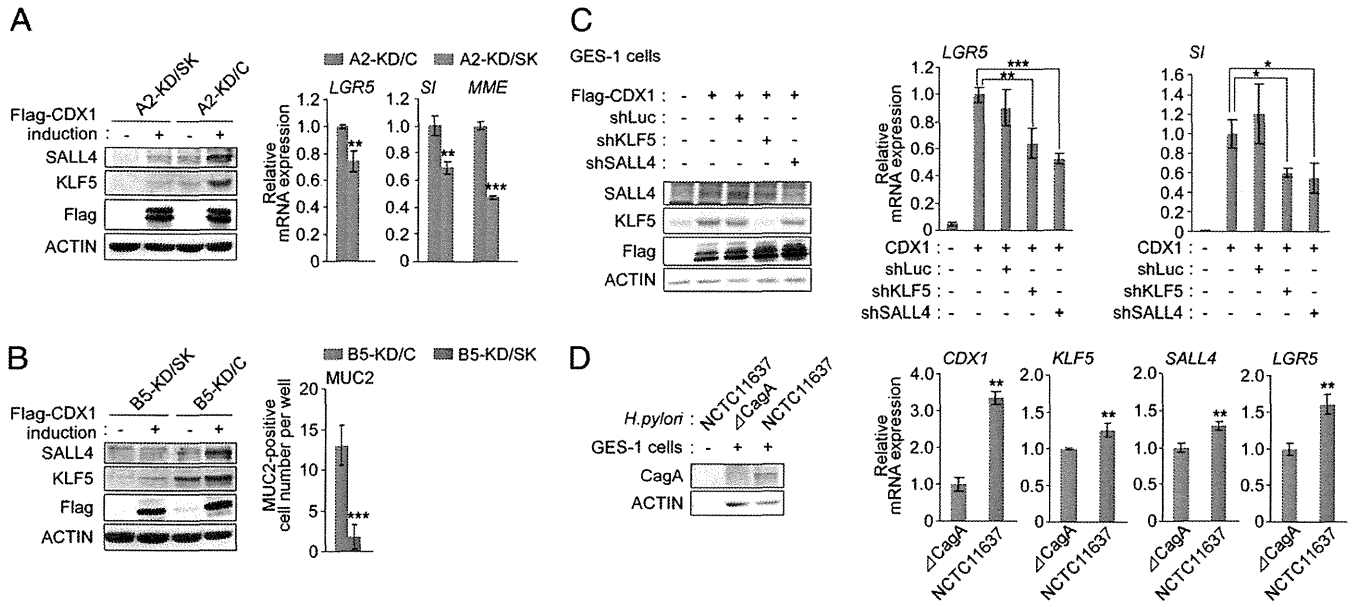

Fig. 6. Involvement of SALL4 and KLF5 in CDX1-mediated intestinal transdifferentiation. (*A* and *B*) MKN28-derived SALL4/KLF5 double-knockdown (A2-KD/SK or B5-KD/SK) or control-knockdown (A2-KD/C or B5-KD/C) cells were induced to express CDX1 by Dox depletion for 24 h. Cell lysates were subjected to immunoblotting with the respective antibodies (*Left*). The mRNA levels for intestinal markers were determined by RT-qPCR in CDX1-induced cells (*A*, *Right*). The number of MUC2$^+$ cells per well in the eight-well chamber slide was counted in CDX1-induced cells (*B*, *Right*). (*C*) GES-1 cells transiently transfected with a Flag-CDX1 vector together with pSUPER-shLuc, pSUPER-shKLF5/1, or pSUPER-shSALL4/1 were cultured for 24 h. Cell lysates were immunoblotted with the respective antibodies (*Left*). Levels of the *LGR5* and SI mRNAs were determined by RT-qPCR (*Right*). (*D*) GES-1 cells infected with *H. pylori* for 24 h were lysed with 0.1% saponin, which disrupts mammalian cells but not bacterial cells. The lysates were then immunoblotted with the respective antibodies (*Left*). RNAs isolated from GES-1 cells infected with *H. pylori* isogenic strains for 96 h were subjected to RT-qPCR analysis for the indicated mRNAs (*Right*). Error bars, ± SD; $n = 3$.

Induction of the intestinal-stemness marker, *LGR5*, by ectopic CDX1 was subdued under the condition of suppression of SALL4 and KLF5 (Fig. 6*A*, *Right*). Expression of intestinal-differentiation markers, *SI* and *MME*, by ectopic CDX1 was much less efficient when the expression of SALL4 and KLF5 was inhibited (Fig. 6*A*, *Right*). The number of MUC2$^+$ cells following prolonged exposure to CDX1 was dramatically decreased upon knockdown of SALL4 and KLF5 (Fig. 6*B*, *Right*). The degree of induction of intestinal-stemness marker and intestinal-differentiation marker by ectopic CDX1 was also reduced when expression of endogenous SALL4 or KLF5 was transiently inhibited in GES-1 cells (Fig. 6*C*). Thus, CDX1-mediated induction of SALL4 and KLF5 plays a critical role in the intestinal transdifferentiation of gastric epithelial cells by establishing an intestinal stem/progenitor-like state, from which various intestinal cell types arise.

We then infected GES-1 cells with a *cagA*$^+$ or a *cagA*$^-$ *H. pylori* isogenic strain (Fig. 6*D*, *Left*). At 96 h after *H. pylori* infection, RNAs were isolated from the cells and subjected to RT-qPCR analysis. The results of the experiment revealed that *H. pylori* infection induced *CDX1* in a *cagA*-dependent manner in GES-1 cells, followed by elevated levels of reprogramming factors, *SALL4* and *KLF5*, and an intestinal stem cell marker, *LGR5* (Fig. 6*D*, *Right*). These observations provided pathophysiological relevance for the ectopic expression of CDX1 in the induction of intestinal metaplasia in patients infected with *H. pylori cagA*$^+$ strains.

Discussion

Chronic infection with *H. pylori* is a major cause of gastric intestinal metaplasia, a precancerous mucosal lesion from which intestinal-type adenocarcinoma arises. CagA, a major virulence factor of *H. pylori* that is delivered into gastric epithelial cells via type IV secretion, aberrantly activates the Wnt/β-catenin signal and ectopically induces Wnt target genes including *CDX1* (8). A causal relationship between ectopic CDX1 and intestinal metaplasia has been provided by the observation that transgenic expression of Cdx1 per se is sufficient to induce intestinal metaplasia in the mouse stomach (9). Persistence of metaplastic changes after removal of triggering agents such as *H. pylori* indicates that expression of a key inducer of metaplasia must have been maintained in the absence of triggering agents. CDX1 fits this idea in that it establishes an autoregulatory network to maintain its own expression (22). However, the mechanism by which ectopic CDX1 provokes metaplastic changes has remained poorly understood.

In intestinal epithelial cells, CDX1 acts as a differentiation-promoting factor (6). Assuming that metaplasia requires the conversion of differentiated cells into less-differentiated states, ectopically expressed CDX1 may also activate stemness-regulating reprogramming factors, which allow dedifferentiation of gastric epithelial cells so that they acquire multipotency characteristic of intestinal stem/progenitor-like cells. Consistently, Cdx1 has recently been reported to be a constituent of the transcriptional network that confers pluripotency on ES cells (23). We found that CDX1 directly induces SALL4, a zinc-finger transcription factor playing an important role in maintaining self-renewal and pluripotency (12). Especially, Sall4 positively regulates *octamer-binding protein 4 (Oct4)*, *c-Myc*, *SRY-box containing gene 2 (Sox2)*, and *Klf4*, the four defined transcription factors capable of generating iPS cells (13). CDX1 also transactivates *KLF5*, a gene encoding a member of the KLF family of transcription factors. Importance of KLFs in the acquisition of pluripotency has been highlighted by recent studies showing that depletion of Klf2, Klf4, and Klf5 in mouse ES cells abolishes self-renewal (24). Furthermore, Klf5 can replace Klf4 in generating iPS cells, indicating a redundant role between KLF4 and KLF5 in stemness induction/maintenance (15). In adult tissues, Sall4 and Klf5 are expressed in hepatic stem cells and hair follicle stem cells, respectively, to maintain tissue stemness (25, 26). Identification of the reprogramming factors SALL4 and KLF5 as direct transcriptional targets of CDX1 therefore provides a mechanistic basis underlying intestinal metaplasia of the stomach. On the one hand, CDX1 activates reprogramming transcription factors in

gastric epithelial cells and thereby rewires transcriptional circuitries so as to redirect gastric epithelial cells toward a less-differentiated intestinal stem/progenitor-like state. On the other hand, CDX1 creates transcriptional circuitries that direct transdifferentiation of dedifferentiated cells into intestinal epithelial cells. Cancer stem cells have recently been reported to possess properties that are shared in common with tissue stem/progenitor cells (27). The observation indicates that acquisition of stemness traits is linked to cell transformation and suggests that a transition through intestinal stem/progenitor-like states via dedifferentiation predisposes cells to undergo neoplastic changes. This may explain the clinical observation that intestinal metaplasia is a precancerous lesion of the stomach (3).

In intestinal epithelial cells, the two homologous CDX1 and CDX2 (Cdx1 and Cdx2 in mice) transactivate a number of intestine-specific genes (6). Like Cdx1, transgenic expression of Cdx2 in the mouse stomach also causes intestinal metaplasia (10), indicating a redundant role of Cdx1 and Cdx2 in the pathogenic change. Interestingly, genomic binding sites for CDX2 include 5′-flanking regions of *SALL4* and *KLF5* (28). It is therefore possible that CDX2 provokes intestinal transdifferentiation via direct activation of *SALL4* and *KLF5*, like CDX1. Also of note, Cdx2 is capable of inducing *Cdx1* mRNA in the mouse stomach (29). Hence, CDX2-mediated intestinal metaplasia might be at least partly due to CDX2-induced CDX1. Whereas CDX-induced intestinal metaplasia is thought to be a precancerous stomach lesion, the potential role of CDX1 or CDX2 in intestinal carcinogenesis remains unclear. Cdx1 and Cdx2 were originally described as an oncoprotein and tumor suppressor, respectively, in intestinal cells (30, 31). However, recent studies suggested that overexpression of Cdx1 has very limited contribution, if any, to the development of intestinal tumors (32, 33). Hence, CDX1 could promote oncogenesis only when it is ectopic expressed in non-intestinal epithelial cells.

The present work provided evidence that ectopic expression of CDX1 and subsequent induction of stemness-associated reprogramming factors SALL4 and KLF5 by CDX1 are key events underlying gastric intestinal metaplasia. As far as we know, this is a unique demonstration of the involvement of reprogramming factors in metaplastic changes. The finding also gives mechanistic insights into intestinal transdifferentiation; CDX1-directed rewiring of transcriptional circuitries through induction of reprogramming factors converts differentiated gastric epithelial cells to immature intestinal stem/progenitor-like cells, which can transdifferentiate into intestinal cells. Reactivation of such reprogramming factors may broadly contribute to the plasticity of the lineage commitment in both physiological and pathological conditions. Our work therefore provides deeper insights into organogenesis and oncogenesis that can be applied to help the progress of regenerative medicine as well as cancer prevention and treatment.

Materials and Methods

The experiments using human materials were approved by the Research Ethics Committee of the Graduate School of Medicine, The University of Tokyo, and the Ethics Committee of Keio University School of Medicine. Informed consent was obtained from all patients. The experiments using animals were approved by the Committee of Experimental Animal Ethics of Jichi Medical University. Cdx1-transgenic mice have been described previously (9). Luciferase reporter assay, qPCR analysis, and cell-counting assay were evaluated using Student's *t* test. $P < 0.05$ was considered to be statistically significant. For all statistical comparisons in these assays, $P < 0.001$ was denoted as ***, $P < 0.01$ as **, and $P < 0.05$ as *. The Gene Expression Omnibus accession number for expression microarray and ChIP-chip analyses in this study is GSE35369. Details of materials and methods are described in *SI Materials and Methods*. Primers used in this study are shown in Table S2.

ACKNOWLEDGMENTS. We thank J. Iovanna, I. Manabe, and R. Nagai for providing plasmids and N. Kamimura, H. Meguro, and D. Sasaya for technical assistance. This work was supported by Grants-in-Aid for the Scientific Research in an Innovative Area from the Ministry of Education, Culture, Sports, Science and Technology (MEXT) of Japan.

1. Gutiérrez-González L, Wright NA (2008) Biology of intestinal metaplasia in 2008: More than a simple phenotypic alteration. *Dig Liver Dis* 40(7):510–522.
2. Reid BJ, Li X, Galipeau PC, Vaughan TL (2010) Barrett's oesophagus and oesophageal adenocarcinoma: Time for a new synthesis. *Nat Rev Cancer* 10(2):87–101.
3. Correa P (1988) A human model of gastric carcinogenesis. *Cancer Res* 48(13):3554–3560.
4. Dearolf CR, Topol J, Parker CS (1989) The *caudal* gene product is a direct activator of *fushi tarazu* transcription during *Drosophila* embryogenesis. *Nature* 341(6240): 340–343.
5. Margalit Y, Yarus S, Shapira E, Gruenbaum Y, Fainsod A (1993) Isolation and characterization of target sequences of the chicken *CdxA* homeobox gene. *Nucleic Acids Res* 21(21):4915–4922.
6. Guo RJ, Suh ER, Lynch JP (2004) The role of Cdx proteins in intestinal development and cancer. *Cancer Biol Ther* 3(7):593–601.
7. Prinos P, et al. (2001) Multiple pathways governing *Cdx1* expression during murine development. *Dev Biol* 239(2):257–269.
8. Murata-Kamiya N, et al. (2007) *Helicobacter pylori* CagA interacts with E-cadherin and deregulates the β-catenin signal that promotes intestinal transdifferentiation in gastric epithelial cells. *Oncogene* 26(32):4617–4626.
9. Mutoh H, et al. (2004) Cdx1 induced intestinal metaplasia in the transgenic mouse stomach: Comparative study with Cdx2 transgenic mice. *Gut* 53(10):1416–1423.
10. Silberg DG, et al. (2002) *Cdx2* ectopic expression induces gastric intestinal metaplasia in transgenic mice. *Gastroenterology* 122(3):689–696.
11. Lapidot M, Mizrahi-Man O, Pilpel Y (2008) Functional characterization of variations on regulatory motifs. *PLoS Genet* 4(3):e1000018.
12. Zhang J, et al. (2006) Sall4 modulates embryonic stem cell pluripotency and early embryonic development by the transcriptional regulation of *Pou5f1*. *Nat Cell Biol* 8(10):1114–1123.
13. Yang J, et al. (2008) Genome-wide analysis reveals Sall4 to be a major regulator of pluripotency in murine-embryonic stem cells. *Proc Natl Acad Sci USA* 105(50):19756–19761.
14. Tsubooka N, et al. (2009) Roles of Sall4 in the generation of pluripotent stem cells from blastocysts and fibroblasts. *Genes Cells* 14(6):683–694.
15. Nakagawa M, et al. (2008) Generation of induced pluripotent stem cells without Myc from mouse and human fibroblasts. *Nat Biotechnol* 26(1):101–106.
16. Conkright MD, Wani MA, Anderson KP, Lingrel JB (1999) A gene encoding an intestinal-enriched member of the Krüppel-like factor family expressed in intestinal epithelial cells. *Nucleic Acids Res* 27(5):1263–1270.
17. Wray GA, et al. (2003) The evolution of transcriptional regulation in eukaryotes. *Mol Biol Evol* 20(9):1377–1419.
18. Qiao XT, et al. (2007) Prospective identification of a multilineage progenitor in murine stomach epithelium. *Gastroenterology* 133(6):1989–1998.
19. Gao X, Sedgwick T, Shi YB, Evans T (1998) Distinct functions are implicated for the GATA-4, -5, and -6 transcription factors in the regulation of intestine epithelial cell differentiation. *Mol Cell Biol* 18(5):2901–2911.
20. Sonoyama K, Rutatip S, Kasai T (2000) Gene expression of activin, activin receptors, and follistatin in intestinal epithelial cells. *Am J Physiol Gastrointest Liver Physiol* 278 (1):G89–G97.
21. Lin SA, Barker N (2011) Gastrointestinal stem cells in self-renewal and cancer. *J Gastroenterol* 46(9):1039–1055.
22. Béland M, et al. (2004) *Cdx1* autoregulation is governed by a novel Cdx1-LEF1 transcription complex. *Mol Cell Biol* 24(11):5028–5038.
23. Kim J, Chu J, Shen X, Wang J, Orkin SH (2008) An extended transcriptional network for pluripotency of embryonic stem cells. *Cell* 132(6):1049–1061.
24. Jiang J, et al. (2008) A core Klf circuitry regulates self-renewal of embryonic stem cells. *Nat Cell Biol* 10(3):353–360.
25. Oikawa T, et al. (2009) Sall4 regulates cell fate decision in fetal hepatic stem/progenitor cells. *Gastroenterology* 136(3):1000–1011.
26. Morris RJ, et al. (2004) Capturing and profiling adult hair follicle stem cells. *Nat Biotechnol* 22(4):411–417.
27. Mani SA, et al. (2008) The epithelial-mesenchymal transition generates cells with properties of stem cells. *Cell* 133(4):704–715.
28. Verzi MP, et al. (2010) TCF4 and CDX2, major transcription factors for intestinal function, converge on the same *cis*-regulatory regions. *Proc Natl Acad Sci USA* 107(34):15157–15162.
29. Mutoh H, Hayakawa H, Sakamoto H, Sashikawa M, Sugano K (2009) Transgenic Cdx2 induces endogenous Cdx1 in intestinal metaplasia of Cdx2-transgenic mouse stomach. *FEBS J* 276(20):5821–5831.
30. Chawengsaksophak K, James R, Hammond VE, Köntgen F, Beck F (1997) Homeosis and intestinal tumours in *Cdx2* mutant mice. *Nature* 386(6620):84–87.
31. Soubeyran P, et al. (2001) Homeobox gene Cdx1 regulates Ras, Rho and PI3 kinase pathways leading to transformation and tumorigenesis of intestinal epithelial cells. *Oncogene* 20(31):4180–4187.
32. Bonhomme C, et al. (2008) *Cdx1*, a dispensable homeobox gene for gut development with limited effect in intestinal cancer. *Oncogene* 27(32):4497–4502.
33. Crissey MA, et al. (2008) The homeodomain transcription factor Cdx1 does not behave as an oncogene in normal mouse intestine. *Neoplasia* 10(1):8–19.

Helicobacter pylori infection in functional dyspepsia

Hidekazu Suzuki and Paul Moayyedi

Abstract | Functional dyspepsia is the most common reason for patients to experience chronic epigastric pain or discomfort. The causes of functional dyspepsia are multifactorial but *Helicobacter pylori* infection is one likely candidate. Infection with this bacterial pathogen clearly results in chronic mucosal inflammation in the stomach and duodenum, which, in turn, might lead to abnormalities in gastroduodenal motility and sensitivity. Chronic gastritis might also affect a variety of endocrine functions of the stomach including the production of the gastrointestinal hormones and neurotransmitters somatostatin, gastrin and ghrelin. Although these abnormalities might generate symptoms in some patients with functional dyspepsia, the clinical evidence needs to be critically evaluated before this hypothesis can be confirmed. A Cochrane review reported that eradication of *H. pylori* in these patients had a small but statistically significant long-term effect on symptom relief when compared with placebo, lasting at least 12 months after 1 week of eradication therapy. The efficacy of eradication therapy was seen in all symptom subtypes of functional dyspepsia, but was more marked in Asian than Western patients. This evidence has led to alterations in most of the major guidelines throughout the world, which now recommend *H. pylori* eradication in patients with functional dyspepsia if they test positive for this bacterium.

Suzuki, H. & Moayyedi, P. *Nat. Rev. Gastroenterol. Hepatol.* **10**, 168–174 (2013); published online 29 January 2013; doi:10.1038/nrgastro.2013.9

Introduction

Dyspepsia refers to a broad range of chronic gastroduodenal symptoms—including pain or discomfort centred in the upper abdomen, early satiety, fullness, bloating sensation in the upper abdomen and nausea—seen commonly in individuals throughout the world.[1] Patients with dyspepsia have a normal life expectancy,[2] but a markedly reduced quality of life[3] and often need to undergo multiple tests to establish the aetiology of their symptoms. Upper gastrointestinal endoscopy findings appear normal in approximately 75% of patients with dyspepsia,[4] and most of these individuals are diagnosed with functional dyspepsia. The treatment of functional dyspepsia remains a challenge, however, as the pathophysiology of the condition is poorly understood.

Multiple theories have been proposed to describe the underlying pathophysiology of functional dyspepsia symptoms, including dysmotility and/or hypersensitivity in the upper gastrointestinal tract.[5] In some cases, these abnormalities might have a postinfectious cause.[6,7] Although a variety of bacterial infections have been implicated in the pathogenesis of this disorder,[8] *H. pylori* is one of the most likely causes, as it is the most common chronic infection worldwide and primarily involves the gastric mucosa. Moreover, large population-based studies have shown that this bacterium is found more frequently in the gastric mucosa of patients with dyspepsia than in that of healthy individuals.[9] Trials conducted to evaluate the efficacy of *H. pylori* eradication treatment for functional dyspepsia have yielded conflicting results, but eradication of this bacterium is suggested to be effective in at least a subset of patients with this disorder.[10,11] This Review outlines the evidence that *H. pylori* is involved in the pathogenesis of functional dyspepsia.

Division of Gastroenterology and Hepatology, Department of Internal Medicine, Keio University School of Medicine, 35 Shinanomachi, Shinjuku-ku, Tokyo 160-8582, Japan (**H. Suzuki**). Farncombe Family Digestive Health Research Institute, Division of Gastroenterology, Department of Medicine, McMaster University, 1280 Main Street West, Hamilton, ON L8S 4K1, Canada (**P. Moayyedi**).

Correspondence to:
H. Suzuki
hsuzuki@a6.keio.jp

Competing interests
H. Suzuki declares associations with the following companies: Astellas, AstraZeneca, Eisai, Otsuka, Daiichi–Sankyo, Dainippon–Sumitomo, Takeda, Tsumura and Zeria. P. Moayyedi declares associations with the following companies: AstraZeneca, Abbott, Pendopharm, Shire and Takeda. See the article online for full details of these relationships.

Pathogenesis

Inflammation and microcirculation

H. pylori colonization evokes a considerable level of inflammation in the gastric mucosa.[12] Reactive oxygen species, which are released from polymorphonuclear neutrophils after activation by *H. pylori* colonization, are potential toxic factors involved in *H. pylori*-induced gastric mucosal injury.[13] Moreover, polymorphonuclear cell infiltration of the gastric mucosa leads to the development of the initial lesions of *H. pylori* infection, namely chronic active gastritis (Figure 1). The inflammation caused by infection with *H. pylori* leads to gastric microcirculatory disturbances including leukocyte rolling, adhesion and extravasation. Moreover, unstable microvascular flow dynamics (such as ischaemia–reperfusion) also promote leukocyte recruitment, generating a vicious cycle between inflammatory lesion formation and further ischaemia-associated